Check for updates

Polymer Composites

WILEY | spe INSPIRING PLASTICS PROFESSIONALS

REVIEW ARTICLE OPEN ACCESS

Interfacial Chemistry Behind Damage Monitoring in Glass Fiber-Reinforced Composites: Attempts and Perspectives

Marta Colombo[1] | Silvia Mostoni[1] | Giulia Fredi[2] | Carol Rodricks[3] | Gerhard Kalinka[3] | Massimiliano Riva[4] | Andrea Vassallo[4] | Barbara Di Credico[1] | Roberto Scotti[1] | Michele Zappalorto[5] | Massimiliano D'Arienzo[1]

[1]Department of Materials Science, INSTM, Milano, Italy | [2]Department of Industrial Engineering, INSTM, University of Trento, Trento, Italy | [3]Department of Polymer Matrix Composites, Bundesanstalt für Materialforschung nd -prüfung (BAM), Berlin, Germany | [4]CRPI Compagnie Riunite Partecipazioni Industriali Srl, Milano, Italy | [5]Department of Management and Engineering, University of Padova, Vicenza, Italy

Correspondence: Silvia Mostoni (silvia.mostoni@unimib.it)

Received: 13 May 2025 | **Revised:** 1 August 2025 | **Accepted:** 2 August 2025

Funding: UNIMIB and CRPI Srl acknowledge funding for an Innovative Industrial Doctoral Program Under the National Recovery and Resilience Plan (PNRR), Mission 4, Component 2 "From Research to Industry," Investment 3.3—of Italian Ministry of University and Research, funded by the European Union—NextGenerationEU.

Keywords: carbon-based filler | electrical and mechanical properties | fiber modification | glass fiber reinforced polymers | interfacial chemistry | structural health monitoring

ABSTRACT

Glass Fiber Reinforced Polymers (GFRPs) are widely used in structural applications but degrade over time due to internal damage. Structural Health Monitoring (SHM) enables early damage detection, improving reliability and reducing maintenance costs. Traditional SHM methods are often invasive and expensive. An emerging solution involves the embedding of carbon-based filler like carbon nanotubes and reduced graphene oxide into GFRPs, forming conductive networks that detect damage through resistance changes. However, poor adhesion among GF, filler, and matrix can reduce mechanical performance. Therefore, tailoring GF and filler surface chemistry is essential to enhance durability and enable effective self-sensing properties. This review summarizes the most recent efforts in modifying GF with carbon-based filler to design GFRP with improved sensing ability and mechanical performance. After a brief introduction on the role of SHM solutions in early damage detection, an overview of the common GF and filler used in GFRPs will be provided. Then, the most relevant GF modification strategies exploited to incorporate carbon-based filler in GFRPs will be described, focusing on the chemical grafting approach, which allows a careful optimization of the fiber/matrix interface. Last, a concise summary of the key mechanical and electrical tests to evaluate interfacial adhesion and self-sensing will be supplied.

1 | Introduction

The use of advanced GFRPs for structural applications has been tremendously growing in the last years due to the thrust of dominating industrial fields like aerospace, automotive, wind energy, and construction industries. Their widespread utilization is connected to their exceptional mechanical properties such as high stiffness and fatigue resistance, given by the integration of reinforcing fibers in the polymeric matrix, and their low production costs, chemical resistance, and design flexibility prompted their diffusion against metal or ceramic materials. In light of these applications, safety and long-term reliability are mandatory requirements for composite materials, which are necessary to guarantee their secure employment. This is particularly relevant when considering a design life of 25 years for a turbine blade or more than 200,000 km for a high-performance car frame. However, obtaining

This is an open access article under the terms of the Creative Commons Attribution License, which permits use, distribution and reproduction in any medium, provided the original work is properly cited.

© 2025 The Author(s). *Polymer Composites* published by Wiley Periodicals LLC on behalf of Society of Plastics Engineers.

Summary

- Conductive fillers in GFRPs act as reinforcements and sensors for damage detection.
- GF surface modification with rGO and CNTs enhances adhesion, electrical, and mechanical properties.
- Physical methods are scalable but struggle with achieving effective filler dispersion and percolation.
- Chemical grafting better improves adhesion and filler distribution, but it is harder to scale up.
- Mechanical and electrical test results for adhesion and self-sensing are tightly connected to the hybrid interface.

high-performance structures is particularly challenging because they are frequently subjected to severe working conditions, such as complex multiaxial cyclic loads, prominent levels of strain or stress, or even exceptional loading conditions. These may induce a continuous decrease in material stiffness and can cause a composite structure to lose up to 30%–40% of its initial stiffness well before the final failure. Besides, defects or damages may occur at any time during the whole lifecycle of GFRPs, namely voids, fibers wrinkling, delamination, or impact damage [1], which concerns the matrix, fiber, and particularly their interfaces.

Thus, early identification of structural damages or potential breakages is necessary to ensure operational safety. Conventional non-destructive testing (NDT), such as visual, ultrasonic, thermographic, infrared thermography, radiographic, electromagnetic testing, and many others [2, 3] are the most widely used analytical technologies to identify failures or defects. However, they rely on a suitable program of periodic inspections to guarantee the monitoring of damage development and remaining lifetime by an external operator, which may result in delayed damage detection and increased costs. To overcome these issues, emerging structural health monitoring techniques have recently demonstrated promising performance by counting on the implementation of in situ damage external detection systems, which behave as real-time sensors and are particularly efficient in the anticipation of structural failures [4]. This becomes even more significant in the presence of internal damage, which cannot be easily detected by the most common methods, such as visual inspection. In general, SHM technologies are based on the use of permanently anchored external sensors or actuators in engineered structures, such as acoustic emission sensors or optical sensors, which acquire real-time responses of composite materials to an external stimulus during service conditions. The working principle of SHM is similar to that of the human body, as the installed sensors are expected to identify the modifications to the structure of the material and to report it to a control center through a transmission unit (Figure 1a), which will elaborate a proper response.

Interestingly, the most recent advancements in the field are driving towards the development of smart SHM materials with self-sensing capabilities that do not involve any external sensors and permit cost, and weight reduction compared to traditional technologies, without using any cable and wires. In this case, the sensing properties for SHM are achieved by the incorporation of conductive fillers in GFRPs, acting both as effective reinforcing fillers and "artificial neurons" for damage detection. In detail, the integration of these materials directly in the epoxy matrix results in the generation of a conductive network. The occurrence of structural damage creates local interruptions in this network, leading to an increase in the measured electrical resistance of the composite material, which can be used as a probe, beyond mechanical tests, to quantify the health state of the materials.

In this context, carbon-based fillers are the most commonly used class of materials to impart the electroconductivity response in the form of carbon black (CB) nanoparticles, carbon nanotubes, graphene nanoplatelets, or reduced graphene oxide, which leads to the formation of a percolative conductive network. Figure 1b illustrates a schematic of self-monitoring in a model GFRP ply, where the dashed red line indicates the conduction path through the percolating filler network. Electrical conductivity is guaranteed by ohmic conduction via contacting filler particles and tunneling conduction across the gaps between particles or agglomerates [5]. During the whole activity, a careful damage analysis of the composites is carried

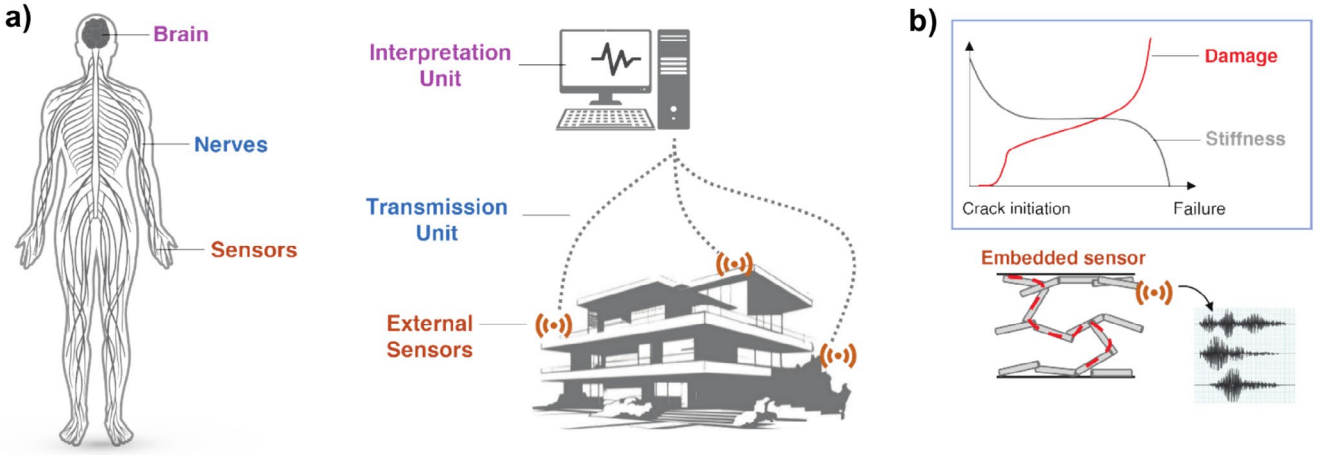


FIGURE 1 | (a) Analogy between the structure of the human body and of smart structures based on SHM; (b) schematic representation of a cross-ply composite with the presence of a conductive filler network and corresponding stiffness loss and increase of the electrical resistance of the composite due to in service loadings. The red dashed line represents the conduction path across the percolative network.

15480569, 0, Downloaded from https://4spepublications.onlinelibrary.wiley.com/doi/10.1002/pc.70332, Wiley Online Library on [26/08/2025]. See the Terms and Conditions (https://onlinelibrary.wiley.com/terms-and-conditions) on Wiley Online Library for rules of use; OA articles are governed by the applicable Creative Commons License

out, with the aim of evaluating the main damage mechanisms (crack initiation, propagation and fiber failure) under static, fatigue, and impact loadings. The self-monitoring performance is then assessed by monitoring the variation in electrical resistance during these mechanical tests, revealing the effect of damage on the electrical properties of the composites and their self-sensing capabilities.

The main advantage of this approach is that it can be considered a non-invasive in situ technology, with high sensitivity to both matrix and interfacial damages, along with high versatility and design flexibility that can be achieved by tuning the filler nature, size, shape, and loadings. These can be embedded in the matrix by exploiting several physical and chemical approaches, that is, by mixing them with the resin, by coating the GF surface, or through chemical grafting. However, the use of proper operational conditions is crucial to determine a significant filler dispersion and distribution; thus, promoting the formation of a suitable conductive network by simultaneously maintaining the mechanical properties of GFRPs.

As mentioned before, one of the most critical factors influencing the progressive damage of these composites is the fiber–filler/matrix interface, where stress concentration occurs due to differences in the thermal expansion coefficients between the GF, the filler, and the polymer phase. Describing the interface concept in the case of GFRP composites is, in fact, not so straightforward. According to Figure 2, at the macroscopic level, the interface can be viewed as the shared boundary between the fibers and the matrix. At the microscopic level, this boundary is a transition zone often referred to as "interphase," where the chemical, physical, and mechanical properties gradually evolve from the fiber to the matrix [6]. In this interphase, the polymer chains can either behave like those of bulk matrix (polymer) or exhibit distinct properties due to their interaction with the fiber surface (i.e., adsorbed material). Moreover, this region is further altered during the composite consolidation or fabrication process as a function also of the fiber topography.

Consequently, tailoring the filler arrangement with respect to the GF and modulating the interphase nanostructure established among the filler, GF, and the polymer play a pivotal role in modulating the fiber/matrix adhesion; thereby opening the possibility of optimizing both the sensing and the mechanical properties of GFRPs [7–9].

Depending on the bonding conditions at the fiber/matrix interface, several adhesion mechanisms may work simultaneously: mechanical interlocking, electrostatic adhesion, interdiffusion, and chemical bonding. For instance, when the fiber surface is rough, mechanical interlocking is more likely to take place at the interface. Electrostatic bonding, on the other hand, results from the attraction between positive and negative charges localized at the surface of the filler and matrix, but it is rarely observed in GFRP. Interdiffusion bonding relies on the ability of polymer chains to diffuse into the interphase region, often forming interpenetrating polymer networks as a transition zone between the bulk matrix and GF. Finally, chemical bonding entails a reaction at the interface of the chemical groups on the GF and filler surface with those of the matrix, forming covalent bonds. The occurrence of these mechanisms is tightly connected to the surface features of fiber, filler, and polymer host.

In particular, the incorporation of carbon-based fillers in GFRPs not only improves their electrical conductivity but also exerts a crucial influence on some of the above-described adhesion mechanisms. For instance, CNTs can significantly increase the surface area available for interaction at the GF/matrix interface, promoting enhanced mechanical interlocking because the roughened surface created by the CNTs on one hand provides additional mechanical anchorage points; on the other hand, it enables the polymer chains to better penetrate and encapsulate the fibers. This increases the load transfer efficiency from the matrix to the fibers. Moreover, as described in Section 4, surface modified CNTs and GO can form strong covalent or van der Waals bonds with both the GF and the polymer matrix, thus enhancing chemical adhesion. It has also to be mentioned that the introduction of nanocomponents improves the wettability of GF, ensuring better impregnation of the matrix into the fiber bundles, strengthening the adhesion forces at the interface, promoting a more uniform distribution of stress, and reducing void content. Finally, CNTs and graphene possess exceptionally high mechanical and electrical conductivity properties so that, when integrated into the fiber/matrix interface, they contribute to the local stiffness and piezoresistive behavior of the composite.

From this background, the next sections will first provide a brief illustration of the main components used to produce GFRPs, namely glass fiber types and polymer matrices; then a detailed description of the characteristics of CNTs and GO filler currently utilized to develop conductive GFRPs will be given.

2 | Basic Components and Manufacturing of GFRPs

The production of GFRPs is based on two main elements, namely the polymer matrix and the glass fibers, which represent the primary skeleton of GFRPs. In these composites, GFs are embedded in a continuous polymeric matrix, acting as reinforcing

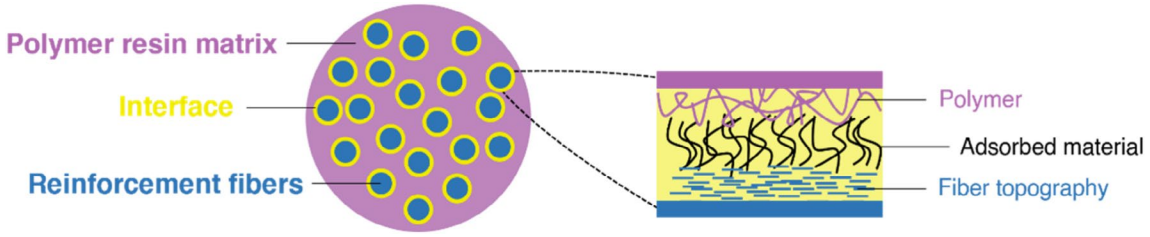


FIGURE 2 | Schematic representation of interface/interphase in GFRPs.

15480569, 0, Downloaded from https://4spepublications.onlinelibrary.wiley.com/doi/10.1002/pc.70332, Wiley Online Library on [26/08/2025]. See the Terms and Conditions (https://onlinelibrary.wiley.com/terms-and-conditions) on Wiley Online Library for rules of use; OA articles are governed by the applicable Creative Commons License

agents and enhancing the mechanical properties of the bare polymer. The selection of raw materials is one of the most crucial steps in the formulation of GFRPs, as it strongly impacts the final application and desired performance. Beyond their nature, several parameters, such as their structural features, shape, volume fraction, and thermal and mechanical resistance, must be considered from an industrial perspective to fulfill the necessary requirements and reach the product application. Moreover, depending on the specific utilization of GFRPs, minor components and/or fillers (i.e., carbon-based or ceramic oxide fillers) as well as organic compatibilizers are added to impart sensing properties or more specific reinforcing features to the composite. In the following section, the main characteristics of the polymer and GFs used for GFRP production are highlighted.

2.1 | Polymer Matrix

The continuous polymeric phase used for GFRPs can be classified as a thermoset or thermoplastic material. Thermoplastic polymers are produced by chain or step growth polymerization of monomers and have a very high molecular weight such as 100,000–250,000 for high density polyethylene (HDPE) or 8000–31,000 for polyethylene terephthalate (PET). In general, these polymers do not require any chemical crosslinking reaction to obtain the desired mechanical features; therefore, they can be dissolved and repeatedly melted or softened by applying heat, allowing re-processability and recycling. However, the high melt viscosity and elevated processing temperature may hinder interfacial interaction and fiber impregnation in the composites, affecting the cost-efficiency and significantly limiting their use in GFRPs.

In contrast, thermoset matrices are widely used for GFRPs production and represent almost 90% of the matrices used in GFRPs. Thermosets are low-molecular-weight resins that require an external stimulus (heat, chemical curing agent, or radiation) to promote the formation of a 3D network through a crosslinking mechanism, depending on the functional groups of the resin chain or hardener agent. This contributes to the thermal and mechanical resistance properties of the polymer, but at the same time results in a complex recycling and reprocessing of the material, due to the impossibility of dissolving the system [10, 11].

The mostly used thermoset polymers in GFRP composites are epoxy, polyester, vinyl ester, and phenolic resins. In particular, epoxy resin is the most widely used thermoset polymer owing to its desirable characteristics, such as resistance to chemicals, good adhesion to different substrates, heat and corrosion resistance, and curing under a wide range of temperatures.

2.2 | Glass Fibers

Among the fiber-reinforced composites for structural applications, GF are the most widely used fibers, thanks to the cheap cost, flexibility, non-magnetic and non-conductive properties, chemical resistance, and the possibility to be molded into complex shapes.

GF are synthetic fiber [12, 13] formed from a silica-based (or other glass) formulation extruded into many fibers with micrometric diameters. According to their nature, fibers can be classified as natural (i.e., jute, flax, cellulose, etc.) or synthetic fibers (i.e., carbon, glass, boron, etc.) [14–16]. The latter impart a higher stiffness, strength, and fatigue strength compared to the natural ones, and show a good compatibility with the polymer matrix, which reduces the fibers aggregation and increases the moisture resistance [17]. For this reason, synthetic fibers and specifically GF have been preferred in industrial applications so far, even though the increasing attention to more recent themes such as renewability, recyclability, and biodegradability is driving the development of more environmentally friendly and low-cost materials [18, 19]. This includes the use of both natural and hybrid fiber-reinforced composites, where two or more types of fiber coexist in a single matrix structure [20]. In fact, natural fibers can be used as a sustainable, renewable, and biodegradable reinforcement in FRPs, but the increment of the mechanical properties of the composite is modest due to their nature. An example is reported by Saleem et al., where ramie and banana fibers are introduced in an epoxy matrix for structural monitoring applications, and the damage mechanism has been evaluated with a non-destructive testing method called acoustic emission testing (AE) [21].

However, GFs remain the most widely used fibers in FRPs and can be categorized based on the fiber length and their chemical composition, that both play a crucial role in determining the specific physical and mechanical properties of the resulting GFRPs. Specifically, the length of the fibers influences their orientation and defines the structural properties of the composite material [22, 23]. In fact, long fiber reinforced composites, called "continuous fiber reinforced composites," are composed by long fibers usually arranged in tows or unidirectional/bidirectional fabrics, leading to an efficient and effective load transfer. On the other hand, shorter fibers, usually in a chopped strand form (3–12 mm) or milled form (0.15–4 mm) [24], termed as "discontinuous fiber reinforced composites," must be carefully chosen to ensure effective load transfer, limit the formation of cracks and, subsequently, avoid the composite failure. In fact, the interfacial weakness and the strength of a composite is directly proportional to the fiber length for the same fiber volume fraction resulting in a non-effective material strength and fracture resistance of the final composite [25]. However, this type of reinforcement is getting attention thanks to the cost-effectiveness, process flexibility, and the potential of achieving isotropic properties. Discontinuous fiber composites bridge the stiffness and strength gap between continuous fiber laminates and neat polymers, which can be interesting, for example, for civil applications (i.e., roadways, concrete structures) where a high degree of wear resistance is required [26], or for automative applications where the processing flexibility and the cost effectiveness are an asset.

Table 1 summarizes the classification of GF according to their chemical composition, where the capital letter (namely E, C, S, A, D, R) is used to differentiate among the percentages of inorganic materials used during their production process.

In general, GF are mainly composed of silica (SiO_2), which represents between 55% and 70% of the whole GF, followed by alumina (Al_2O_3) and a variety of other metal oxides, whose usage is related to a fine control of the resulting mechanical and electrical features, as well as their corrosion resistance. In particular, E-glass

15480569, 0, Downloaded from https://4spepublications.onlinelibrary.wiley.com/doi/10.1002/pc.70332, Wiley Online Library on [26/08/2025]. See the Terms and Conditions (https://onlinelibrary.wiley.com/terms-and-conditions) on Wiley Online Library for rules of use; OA articles are governed by the applicable Creative Commons License

fibers are composed mainly of SiO_2, CaO, and Al_2O_3. They are characterized by good strength, high thermal resistance, and electrical resistivity. In addition, E-glass fibers are distinguished by a strong resistance to the most common chemical agents, to abrasion and vibration, and have excellent flexibility. These characteristics make them the most common type of GF employed in GFRPs.

Generally, the strength of glass fiber is affected by its surface features. The surface concentrations of different oxides in GF can differ from the bulk composition, depending on factors such as the glass thermal history, ambient humidity, and any surface treatments applied after melting and cooling. For instance, E-glass fibers possess other hydroxyl groups, such as Al–OH and B–OH at the surface, besides common silanols (i.e., ≡SiOH) [28–30]. The presence of boron on silica surfaces is known to enhance the reactivity of surface silanol groups with the silanes [31, 32], which is essential for the sizing procedures and for the fabrication of GFRPs (see Section 4.2).

Despite the many benefits, GFs also carry some disadvantages such as their lower stiffness-to-density ratio compared to carbon fibers and, as previously mentioned, their challenging disposal at the end of their service life [26]. In fact, GFRPs, deriving from many stages of manufacturing, cannot be easily recycled or reutilized, and for this reason a lot of research is now facing their waste disposal method [33–35]. Nowadays, the direct reuse of the fibers can be exploited through mechanical grinding, and the chopped fibers are employed in different applications as fillers; on the other hand, chemical and thermal methodologies have been widely studied to recover GFRPs. However, these processes still have negative environmental impacts and high additional costs due to the consumption of high energy required to reach extremely elevated temperatures [36].

2.3 | Manufacturing Techniques of GFRPs

The main techniques utilized for the production of GFRPs, with a special focus on thermosetting matrices, are summarized and schematized in Figure 3.

Different manufacturing protocols have been reported for the preparation of GFRP composites, including hand lay-up [37], resin transfer molding (RTM) [38], vacuum-assisted resin transfer molding (VARTM) [39, 40], filament winding [41], pultrusion [42], compression molding [43], and automated fiber placement (AFP) [44–46]. The choice of one technique over the others is influenced by the production costs and the desired characteristics

TABLE 1 | Chemical compositions (expressed as weight percentages) and physical properties of different glass fibers [27].

Type	SiO_2	Al_2O_3	TiO_2	B_2O_3	CaO	MgO	Na_2O	K_2O	Properties
E-glass	55, 0	14, 0	0, 2	7, 0	22, 0	1, 0	0, 5	0, 3	Higher strength and electrical resistivity
C-glass	64, 6	4, 1	—	5, 0	13, 4	3, 3	9, 6	0, 5	Higher corrosion resistance
S-glass	65, 0	25, 0	—	—	—	10, 0	—	—	Highest tensile strength
A-glass	67, 5	3, 5	—	1, 5	6, 5	4, 5	13, 5	3, 0	Higher durability, strength and electric resistivity
D-glass	74, 0	—	—	22, 5	—	—	1, 5	2, 0	Low dielectric constant
R-glass	60, 0	24, 0	—	—	9, 0	6, 0	0, 5	0, 1	Higher strength and acid corrosion resistance

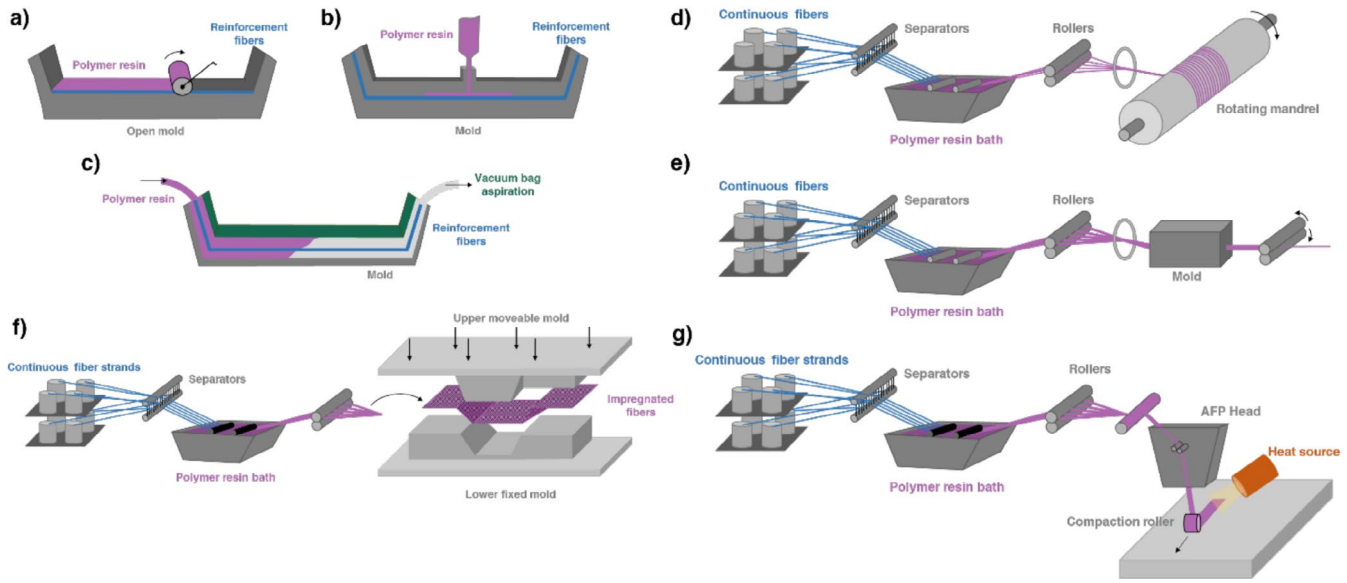


FIGURE 3 | Schematic representation of the manufacturing techniques of GFRPs: (a) hand lay-up, (b) resin transfer molding (RTM), (c) vacuum-assisted resin transfer molding (VARTM), (d) filament winding, (e) pultrusion, (f) compression molding, (g) automated fiber placement (AFP).

15480569, 0, Downloaded from https://4spepublications.onlinelibrary.wiley.com/doi/10.1002/pc.70332, Wiley Online Library on [26/08/2025]. See the Terms and Conditions (https://onlinelibrary.wiley.com/terms-and-conditions) on Wiley Online Library for rules of use; OA articles are governed by the applicable Creative Commons License

of the final composite, such as size, geometry, or mechanical properties. The differences in the methods lie in the experimental techniques used to overlap the polymer matrix and the fibers (i.e., open mold, two-sides mold, polymer resin bath, etc.), as well as in the curing procedure.

3 | Carbon-Based Filler for Imparting Self-Sensing Properties to GFRPs

Recently, the development of smart polymer composites, that is, materials that can react to external stimuli and fluctuations, is gaining popularity thanks to their exceptional properties and various applications. Among them, self-sensing and self-healing materials are known as two responsive classes of materials to detect the damage intrinsically and to reconstruct them, respectively. This is often based on the inclusion of inorganic nanoparticles in the matrix, which not only behave as reinforcing fillers for the composites and enhance their mechanical properties but can also impart additional features.

In this field, traditional GFRPs can be converted to smart polymer composites with self-sensing capabilities thanks to the addition of conductive fillers that are responsible for the formation of a conductive network inside the polymer matrix. Specifically, carbon-based fillers are commonly used to improve the mechanical properties of the composite while also providing electrical conductivity, which is useful for monitoring the health of the composite during its service life.

Among them, the most exploited filler is CB, introduced in the matrix to enhance the overall properties of the polymers, also increasing the abrasion resistance [5, 47–49]. However, the obtained electrical properties are strongly affected by its dispersion and by the generated filler-filler or filler-matrix interactions [50, 51]. For this reason, researchers are more recently exploiting carbon-based allotrope fillers such as CNTs, GO, and its derivatives, as described in the next paragraphs.

3.1 | CNTs: Structure and Properties

CNTs are carbon-based materials composed of a single graphitic sheet (graphene) wrapped in a cylindrical shape, having a diameter in the nanometric scale and a length that can extend to the micrometric scale or more [52]. In general, they can be formed either by a single wall of carbon, namely single-walled CNTs (SWCNTs), or by multiple walls where the cylinders are concentrically organized, giving rise to multi-walled CNTs (MWCNTs). Compared to other carbonaceous fillers and to CB, they show a high aspect ratio and promising structural and functional properties, such as high mechanical strength and electrical conductivity [53]. In fact, CNTs, thanks to the sp^2 bonds between the carbon atoms, show a very high tensile strength and low electrical resistivity, which can be increased by the presence of structural defects [54]. Moreover, they exhibit remarkable elasticity, which enables them to return to their original shape after the removal of the external strain force. Therefore, they have been applied as reinforcing agents for the preparation of composite materials to develop ultra-lightweight and extremely strong materials [55].

In addition, they own electrical and thermal conductivity (10^6–$10^7\,Sm^{-1}$ and 3000–3500 $Wm^{-1}K^{-1}$, respectively [56]) thanks to the strong bonds between the carbon atoms, which allow nanotubes to withstand high electric currents and high temperatures. Thus, they can be used in polymeric composite materials to impart electrical properties, that are strongly influenced by the CNTs concentration, alignment, morphology as well as dispersion due to filler–matrix interactions. Interestingly, their physical shape and resulting structure play a key role in tailoring the resulting electrical, thermal, and structural properties, and can provide a more "metallic" (highly conducting) or semiconductor behavior. In fact, the SWCNTs structure can be designed according to the rolling direction of the graphene in three different ways resumed in Figure 4 (armchair, chiral and zigzag [57, 58]) and can be represented by a vector called chiral vector, $\overrightarrow{C_h}$, where $\overrightarrow{C_h} = n\overrightarrow{a_1} + m\overrightarrow{a_2} = (n, m)$. Among them, armchair CNTs show metallic properties, whereas zig-zag and chiral structures may have different band gap energies depending on their diameter and may span from metals up to semiconductor materials [59].

Regarding MWCNTs, two different structural models can be described: the Parchment model, in which a single nanotube is rolled around itself multiple times, and the Russian Doll model, in which a SWCNT contains another nanotube with a smaller diameter. In the last model, the interlayer distance is similar to the distance between graphene layers in graphite, while the high electrical conductivity is the same for both models. MWCNTs have similar properties to SWCNTs; however, the first have a higher tensile strength, and the protection of the inner carbon nanotubes results in a higher preservation of the structure from chemical interactions [60].

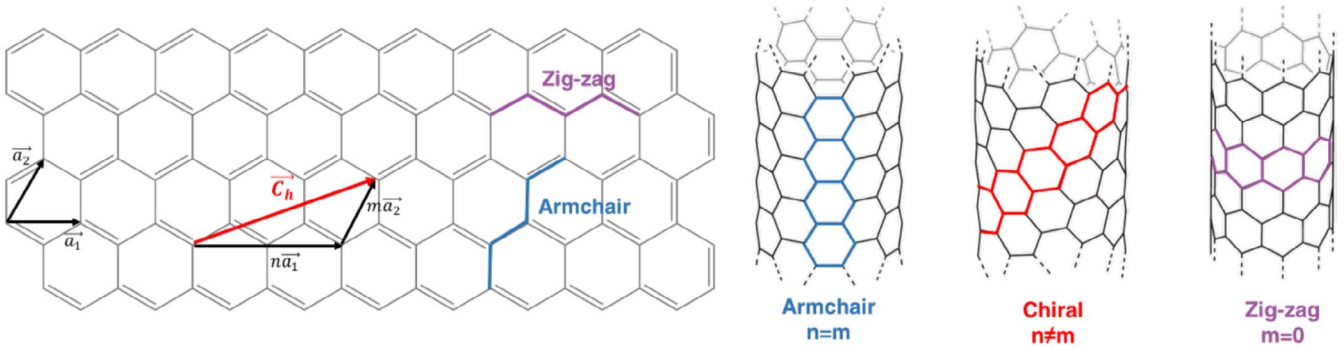


FIGURE 4 | Schematic representation of the chiral vector and the three structures of SWCNTs [57, 58].

15480569, 0, Downloaded from https://4spepublications.onlinelibrary.wiley.com/doi/10.1002/pc.70332, Wiley Online Library on [26/08/2025]. See the Terms and Conditions (https://onlinelibrary.wiley.com/terms-and-conditions) on Wiley Online Library for rules of use; OA articles are governed by the applicable Creative Commons License

CNTs can be mainly synthesized by three methods: arc discharge [61–64], laser ablation [65, 66], and chemical vapor deposition (CVD) [67–69]. The common feature for all these syntheses is the addition of energy to a carbon source, in the presence of a catalyst, to produce groups or single C atoms that recombine to form CNT. The source of energy required for the process may be heat from a furnace for CVD, high-intensity laser for laser ablation, or electricity for arc discharge. The choice of one specific technique can significantly affect some morphological features of SWCNTs and MWCNTs, such as the inner/outer diameter, the length of the nanotube, the control on the size, and the purity of the final product. Consequently, the mechanical and electrical properties of CNT are also affected by the selection of one production method due to the possible presence of structural defects on the surface [70, 71]. Moreover, the choice of the carbon source is a crucial point also for complying with potential environmental issues. In fact, for arc discharge and laser ablation, the source is graphite, while for CVD production, the carbon source can be fossil-based hydrocarbon and plant-based hydrocarbon. Natural gas became the most used carbon source for CNTs production, but also acetylene, benzene, xylene, and toluene. In this case, the carbon source is related to fossil fuels, involving insufficient availability and environmental effects, resulting in efforts to consider using non-petroleum products. On the other hand, natural precursors are rare but attractive thanks to the lower cost and environmental effects. A possibility is to use nondegradable polymers such as turpentine oil, eucalyptus oil, castor oil, coconut oil, and palm oil. Also, waste cooking oil (i.e., palm oil), which is less expensive than virgin oil, is a promising alternative for CNT production [72].

CNTs have been widely used as reinforcement in GFRPs to enhance the mechanical properties of the composite. Panchagnula et al. [73] introduced MWCNTs in an epoxy matrix by ball milling mixing. Tailoring the loading up to 0.4 wt%, the tensile strength increased significantly in accordance with the hardness values. In another work [74], CNTs have been grafted on GF surface with CVD technique exploiting different temperatures. The tensile strength was lower than that of the GF due to limited thermal degradation of the fiber. However, the CNT-grafted GF resulted in an increase in the interlaminar shear strength (ILSS), caused by CNT bridging, maintaining the tensile properties of the composite and improving flexural properties. Moreover, the extremely high electrical conductivity of CNTs has been exploited for applications as self-sensing in GFRP composites [75–78].

3.2 | Graphene and Its Derivates

Graphene is a single graphitic sheet that can be obtained through top-down and bottom-up techniques [79]. In top-down methods, graphene is mainly exfoliated from graphite with a very high yield compared to bottom-up methods, where graphene is deposited on a specific substrate through different processes (i.e., CVD, Plasma enhanced CVD, epitaxial growth in silicon carbide substrate) [80]. The bottom-up technique offers the advantage of a contamination-free product with control over growth, even if it has a very low yield and higher cost for large-scale production.

One main issue related to graphene sheets is that they are usually unstable and tend to agglomerate through van der Waals interactions to form graphite, which is a more stable structure. To solve this concern, graphene can be obtained from the reduction of graphene oxide. GO is an atomic sheet of graphite decorated with oxygenated functional groups on the basal planes and edges with a structure of mixed sp^2 and sp^3 hybridized carbon atoms. GO can be easily synthesized by the oxidation of graphite (and especially graphite oxide), whose added functional groups help the exfoliation process into monolayers of GO by simple stirring or mild sonication. However, as the complete reduction of GO to graphene cannot be achieved, the structure and properties of graphene can be restored by reducing GO to rGO (Figure 5).

The reduction can be made by chemical reactants, thermal, or electrochemical processes [81–84]. In the case of thermal reduction at elevated temperatures, an inert atmosphere is generally required to avoid the combustion of the sample. For the chemical reduction, the widely used reactants are toxic and/or explosive (i.e., hydrazine hydrate, sodium borohydride) [85]. Consequently, in order to alleviate environmental issues, in the last years eco-friendly options have been exploited such as metals (Zinc, iron, and aluminum) [86–88], alkaline solutions (sodium or potassium, hydroxide) [89], sugars (glucose, fructose, and natural cellulose) [90, 91] and other substances [92, 93]. However, the problem of metal contamination and low deoxygenation challenges the development of greener reduction processes. A promising option consists in the utilization of L-ascorbic acid, available in plants and food, as a green, effective, and low-cost alternative reduction agent [94].

Owing to its extremely lightness and inherent strength, graphene can be exploited as filler in polymeric composites, resulting in good mechanical properties [95–98]. Moreover, its most beneficial characteristic is the extremely high electrical

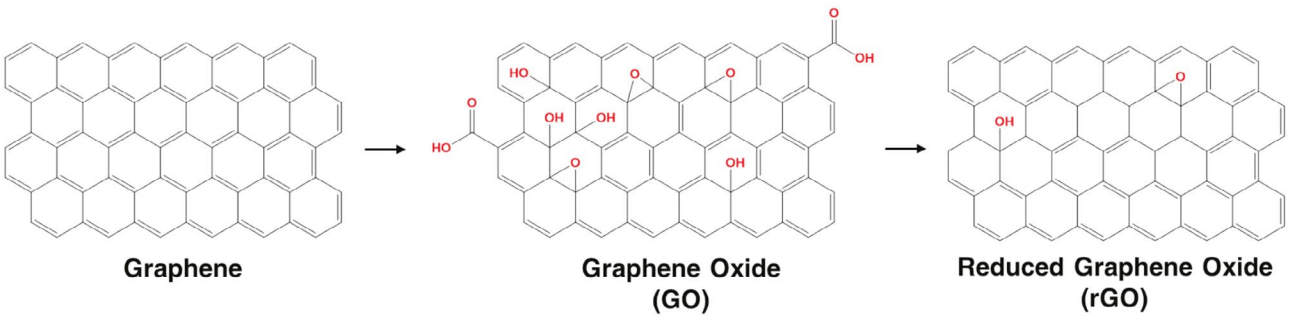


FIGURE 5 | Schematic representation of the structure of graphene, GO, and rGO.

15480569, 0, Downloaded from https://4spepublications.onlinelibrary.wiley.com/doi/10.1002/pc.70332, Wiley Online Library on [26/08/2025]. See the Terms and Conditions (https://onlinelibrary.wiley.com/terms-and-conditions) on Wiley Online Library for rules of use; OA articles are governed by the applicable Creative Commons License

conductivity deriving from the zero-overlap between the conduction and the valence bands (semimetal) that promotes its use for self-monitoring health applications; although the costs are high [99–101].

On the other hand, rGO is a lower-quality product compared to pristine graphene due to the presence of structural defects and residual heteroatoms. However, it is considered a remarkably interesting material thanks to the same characteristics as graphene (good electrical conductivity, etc.) and it is already in use in a lot of applications instead of graphene (i.e., sensors, composite materials). In fact, several examples report the use of rGO as filler in GFRPs enhancing the mechanical properties of the final composite [102–104]. Moreover, scientists are exploiting the introduction of this carbon-based filler in GFRPs for applications in structural monitoring, with the aim to develop a smart material with enhanced mechanical features and high conductivity [105–108].

The next section covers the most relevant strategies for incorporating carbon-based conductive fillers in GFRPs, with a special focus on the GF surface modification by chemical grafting approaches, which warrant careful optimization of the fiber/matrix interface.

4 | Incorporation of CNTs and rGO in GFRPs Composites

As discussed in the previous section, the introduction of carbon structures in GFRPs enhances the mechanical performance of the polymer and imparts useful properties (e.g., electrical conductivity), which are of fundamental importance for specific applications, like structural health monitoring.

To create an electrical conductive pathway to impart self-sensing capabilities in GFRPs, the loading of carbon filler must reach the percolation threshold, that is, the point at which a material undergoes an insulator to conductor transition due to the formation of a 3D conductive network in the polymer matrix. In particular, CNTs, due to their high aspect ratio, often exhibit lower percolation thresholds, typically around 0.01–1 wt%; while rGO can have a wider range, often between 0.1–2 wt%, depending on the degree of exfoliation and processing [109].

The good dispersion of the filler is crucial to obtaining a suitable percolative network. This is particularly relevant in the presence of nanometric filler, whose dimension is comparable to the domains of entangled polymer chains and responsible for a high degree of interaction at the molecular scale [110]. For this reason, reducing the filler aggregation, while enhancing its interactions with the matrix, is of paramount importance to promote their utilization and the further development of self-monitoring materials up to the industrial scale. To this purpose, controlling the chemical and physical properties of the filler/matrix interface is crucial to assure good homogeneity of the resulting composites. In the literature, several methods have been proposed to include carbon-based fillers in GFRPs, such as matrix modification by mechanical mixing [111] or fibers modification through physical, chemical, thermal treatments, and by coating processes [112–115].

4.1 | Matrix Modification

Using this method, carbon-based fillers are pre-dispersed in the resin, and then the composites with GF are prepared using one of the manufacturing techniques described in Chapter 2. However, the main issues of this procedure are related to achieving an optimal dispersion of the nanofiller in the matrix, avoiding the filler aggregation and an excess rise in the matrix viscosity. In fact, graphene and its derivates have a very strong van der Walls forces and π–π interactions between the lamellae, while the high aspect ratio of CNTs leads to the formation of aggregates [116–118]. Consequently, good tailoring of the filler loading is strongly necessary. To this purpose, physical dispersion methods, such as ultrasonication or three-roll-mill machines, can be used to break up aggregates, increasing the homogeneity of the dispersion and avoiding aggregates with dimensions larger than the gaps between fibers tows.

From an industrial point of view, both mechanical and chemical methods have been exploited as scalable and economic approaches to incorporate carbon-based filler in GFRPs [99]. Mechanical dispersion involves solution mixing and melt blending strategies. The first one requires the use of a solvent to introduce the filler in the matrix, which results in a less viscous filler-matrix dispersion allowing easier intercalation between the polymer chains and the layers of the carbon-based filler. A problem can arise during the solvent evaporation process, resulting in trapped air bubbles in the composite, thus reducing the final mechanical properties. Instead, the melt blending appears as a more environmental and economical alternative, since it is a solvent-free approach. The carbon-based filler is included in the matrix with a twin-screw extruder, resulting in intercalated or exfoliated polymer chains. The main issue of the strategy lies in the difficulty of achieving a homogeneous dispersion in a viscous medium as the matrix of the composite.

The chemical dispersion method consists of an in situ polymerization where the conductive filler is dispersed in a solution of monomer followed by a polymerization reaction. This approach allows the formation of covalent or non-covalent bonds between the filler and the matrix, which hinder direct contact among the conductive units and reduce the effects connected to their high aspect ratio.

Kim et al. [119] performed a comparison of the different dispersion methods. Solution mixing results as the best approach for obtaining a remarkable filler distribution in the composite, while melt blending, despite guaranteeing a homogeneous distribution, leads to a significant size reduction and structural distortion of the carbon-based materials. The in situ polymerization approach preserves the diameter of GO sheets, but the formation of a strongly cross-linked filler-matrix network hinders the generation of additional hydrogen bonds between the polymer chains, resulting in limited physical properties of the composite.

4.2 | Fibers Modification

Another common approach to introduce carbon filler is based on the modification of the fibers either by coating or chemical grafting. The surface properties of GF must be suitable for further interactions with the carbon-based materials to obtain valuable and

15480569, 0, Downloaded from https://4spepublications.onlinelibrary.wiley.com/doi/10.1002/pc.70332, Wiley Online Library on [26/08/2025]. See the Terms and Conditions (https://onlinelibrary.wiley.com/terms-and-conditions) on Wiley Online Library for rules of use; OA articles are governed by the applicable Creative Commons License

stable GF modification. In fact, GFs are generally characterized by suitable surface sizing (alkoxysilane with a general formula $(OR)_3Si\text{-}R_2$), applied to prevent fiber damage during processing and improve interfacial compatibility with the resin. Fiber sizing is a complex slurry formulation that can include 10 or more components. The principal ones are film formers and silane coupling agents, but also lubricants, antistatic agents, and surfactants are generally enclosed [120–123]. The benefits of sizing modification include cost-effective and efficient manufacturing of composite materials with improved adhesion at the GF/matrix interface, enhanced short- and long-term performance, and protection of the fiber surface from damage, environmental, and moisture absorption. However, to improve the surface interactions with the applied carbon filler, it is convenient to either remove the GF sizing through previous suitable treatments or exploit oxidative processes on the carbon filler to increase its interaction with the GFs. Examples are provided in the following subsections.

4.3 | Fiber Coating

Coating represents a process of modification of the GF surface with a fixed number of layers of a carbon-based filler suspension, where the stability of the dispersion plays a key role in obtaining a homogeneous film. It can be realized through different techniques, like dip-coating [124–131], doctor blade coating [132], CVD [133–135], electrophoretic deposition (EPD) [136–141], and spray-coating [142–144]. A brief description of all the techniques is provided here.

4.3.1 | Dip-Coating

This method is an industrially developed process based on a simple and scalable setup. It allows good control of the thickness and homogeneity of the film by tailoring the experimental conditions, that is, submersion time, withdrawal speed, number of dipping cycles, solution composition, concentration, and temperature. However, this approach raises environmental concern due to the need for a large reservoir of excess material. Several attempts have been made, especially with CNTs. Uribe-Riestra et al. [125] dip-coated GF in a CNTs suspension to impart electrical properties to the final GFRP composite, aiming for the detection of non-visible damages inside a composite subjected to bending loads. To increase the affinity with the sizing of the GF, they previously oxidized CNTs through an acidic treatment generating surface oxygenated groups. Then a CNTs/distilled water solution was prepared, and the GF weave was dipped in the suspension and dried in an oven at 100°C. The carbon film showed good homogeneity; the weight of CNTs on the fiber surface was approximately 0.5 wt% and the electrical resistance was within the 10^3–$10^4\,\Omega$ range. In another study [130] the suspension of the carbon-based filler was achieved by mixing the rGO powder directly in the epoxy resin. The GF yarns, pretreated with acetone to remove sizing agents and impurities, were dipped in the rGO modified matrix and hung at room temperature to eliminate any excess, achieving a more homogeneous coating and lastly cured at 110°C. The piezoresistive response of the rGO coated fibers exhibited a linear variation under low deformation, suggesting a potential application for damage monitoring. The main disadvantage of dip-coating is the absence of control of the uniformity and smoothness of the surface, which highly affects the electrical conductivity of the final composite [145]. Moreover, this physical coating does not allow modifying significantly the interphase region, because the nature of the fiber/carbon-based filler interaction is mostly electrostatic, potentially resulting in leaching phenomena in the epoxy with detrimental effects on the interfacial adhesion.

4.3.2 | Doctor Blade Coating

This process involves the use of a blade to deposit a coating of solution over a surface. The main advantages compared to dip coating are the consumption of a lower amount of coating material and the well-defined control over the film thickness by adjusting the distance between the sharp blade and the surface. As the movement of the blade is in-line with the surface and removes the excess material, a uniform thickness of the coating film is achieved. On the other hand, a disadvantage is the restricted application to plane substrates only. Moreover, this technique is used to coat a manufactured laminate GF/epoxy without providing the possibility to tune chemically the interphase properties. One significant example in the literature is proposed by Paleari et al. [5], who used MWCNTs to coat GF for structural monitoring applications by doctor blade. Different loadings of MWCNTs (0.75 and 1 wt%) were dispersed in ethanol via sonication before the addition of the resin monomer; after the evaporation of the solvent, the curing agent was added, and the mixture was mechanically stirred. The filled resin was then deposited on glass woven fabrics through a moving blade generating a thin coating. The electrical resistance variation followed a linear trend with the increase of the carbon-based filler loading. The authors suppose that tunneling was the predominant mechanism of conductivity as shown at the lower loading. However, in the 1 wt% CNTs case, the higher filler content was responsible for a percolating system where the ohmic conduction was prevalent.

4.3.3 | CVD

It refers to the deposition of a chemical gas reacting on a surface to form a stable coating in an activated environment like heat or plasma to obtain a high-quality film. Among the various attempts, He et al. [146] studied the design of multifunctional GRFPs by tailoring CNTs geometry to promote GFRPs applications such as structural monitoring, electromagnetic adsorption, de-icing, etc. In this study, CVD was carried out to grow CNTs on the surface of GF. Each GF was covered by a shell of aligned perpendicularly distributed CNTs with a length of 2.5 μm and a diameter between 10 and 20 nm. This orderly arrangement can facilitate the manufacturing process of the composite, promoting the resin diffusion by capillary force, resulting in increased electrical conductivity, improved strength, and remarkable storage and flexural moduli. In fact, the preserved alignment of CNTs anchored to the GF surface boosts the interfacial interactions between the fibers and the matrix. Nevertheless, this process is disadvantageous for GFRPs due to the high temperature required for the deposition (600°C–1000°C) of the carbon-based coating [147] as well as due to the high cost and complicated setup required for scale-up production. Moreover, while this technique provides the convenience of coating fibers with a uniform distribution of nanoparticles, it has the drawback of poor wettability between the inert surfaces

15480569, 0, Downloaded from https://4spepublications.onlinelibrary.wiley.com/doi/10.1002/pc.70332, Wiley Online Library on [26/08/2025]. See the Terms and Conditions (https://onlinelibrary.wiley.com/terms-and-conditions) on Wiley Online Library for rules of use; OA articles are governed by the applicable Creative Commons License

of the fibers and the catalyst precursor, necessary to promote the CNT growth [148, 149], as well as degradation of the fiber's mechanical properties [135, 150].

4.3.4 | EPD

This industrial process involves the suspension of charged particles in a liquid medium that migrate under the influence of an electric field and then deposit onto the surface of an electrode. All colloidal particles with a charged surface can be used for this type of coating, with the GF mounted on the anode. The most relevant problem is the stability of particle dispersion, which involves the choice of a suitable solvent. Moreover, this process is inherently difficult because of the setup organization, as only the side of the fiber or fabric facing the suspension is coated, thus requiring more cycles to obtain a uniform coating. Mahmood et al. [138] exploited EPD to produce piezoresistive composite for strain/damage monitoring. In this work the authors systematically evaluated different concentration of GO solution (0.005–0.2 wt%) and different electric field intensities (0.5–1.5 V cm^{-1}). After deposition, the covered fibers were dried and then subjected to a reduction to obtain rGO and increase the conductivity of the fibers. The rGO coating interphase increased the storage and loss moduli, flexural strength (+23%), and interlaminar shear strength (ILSS) (+29%) of the composites. Furthermore, final composite showed an electrical resistivity of $\sim 10^1\,\Omega\,m$. In another study [137], the authors coated GF surface with MWCNTs through an EPD for in situ mechanical sensor applications. The EPD fibers achieved higher interfacial shear strength without degradation of the fiber strength.

However, this technique carries some disadvantages. Working with nanoparticles introduce the possibility to have an unstable suspension with nanoparticles agglomeration caused by their high specific aera. Moreover, at high electric field the particles do not have enough time to rearrange and well-pack resulting in a limited deposit density [151]. Additionally, this physical coating does not allow entirely the durable modification of the interphase, because of the weak interaction between carbon-based filler and glass surface, which results in filler detachment upon GF introduction in the matrix. A careful tailoring of the parameters of EPD and a pre-impregnation of the GF with the epoxy are essential to obtain the modification of the interface and, consequently, to foster the enhancement of the mechanical properties of the composite [72].

4.3.5 | Spray Coating

This simple method is used to cover irregular surfaces using an airbrush gun connected to an air compressor. Carbon-based filler needs to be stabilized in the suspension to obtain better coating quality, and the concentration of the suspension plays a critical role to avoid the nozzle occlusion. Zhang et al. [142] developed a hybrid composite system by coating carbon fiber prepreg with CNTs to enhance the damage sensing capability and improve the fracture toughness. Two spray parameters were tailored in the process, that is, the air pressure (30 psi) and the distance between the spraying nozzle and the substrate (10 cm). The CNTs were dispersed in methanol by sonication and then sprayed on the carbon fiber prepregs placed perpendicular to the airbrush. Mode-I fracture toughness was significantly improved by 50% by adding a very low CNT loading (0.047 wt%). In a different study [152], both fiber and matrix modification were exploited for a simultaneous reinforcement by introducing different carbon-based fillers (MWCNTs, graphene nanoplatelets [GNPs], GO, and rGO). Briefly, the filler was dispersed in acetone, and part of the solution was sprayed on the fibers. The remaining part was added to the resin. After solvent evaporation, the curing agent was added, and the mixture was used as infusion epoxy for the manufacturing of laminates. Compared to the neat GF/epoxy system, the average ILSS increased by up to 15.4%, 8.9%, 13.3%, and 10.7% with the 0.15, 0.2, 1.0, and 0.042 wt% of MWCNTs, GNP, GO, and rGO, respectively. The main disadvantage of spray coating is the limited thickness control, which usually ends up with not homogeneous coverage of the surface or manifestation of agglomerates. Furthermore, the modification of the GF surface is performed through weak physical interactions leading to a not significant implementation of the interface chemical bond with the matrix.

A concise summary of all the above-described methods is schematized in Figure 6.

4.4 | Chemical Grafting

As reported in the first chapter, the fiber/epoxy interface plays a key role in GFRPs because good interfacial properties are necessary to ensure efficient load transfer. In the absence of primary bonds between these two components, the intermolecular forces of attraction are London and polar forces or acid–base interactions. These secondary forces lead to the degradation of the mechanical properties of the composite under wet conditions because of the diffusion of water molecules to the interface, which replace polymer chains. Subsequently, the presence of compatibilizing agents is essential to improve interfacial adhesion in GFRPs [153]. Organofunctional silanes are the most widely used coupling agents in GFRPs. Their effectiveness relies on several factors, such as the type of silane, the thickness of the silane layer, and the pretreatment of the substrate. However, under wet conditions, the most important aspect is the chemical bonding between the silane and the constituents of the composite (i.e., glass fibers and epoxy matrix). A scheme of the formation of a siloxane thin film through hydrolysis and condensation processes is shown in Scheme 1.

The silane coupling agents hydrolyze to form silanol groups and some oligomers, which then undergo, through an acid or base catalysis, condensation with the OH terminal groups on the glass fiber surface, forming a siloxane bond [154]. At first, silanes can interact with the GF surface by forming hydrogen bonds with the available hydroxyl groups (see Scheme 1). This is typically followed by a condensation reaction that forms siloxane bonds anchoring the silanes to the surface. In some cases, lateral oligomerization may occur without creating direct bonds to the surface [154]. Regardless of the exact mechanism of silane grafting, the resulting siloxane layer on the substrate usually comprises several stacked siloxane layers [155].

Understanding the kinetics and thermodynamics of this process is crucial for controlling the properties of the resulting modified surface. Hydrolysis kinetics have been extensively investigated,

15480569, 0, Downloaded from https://4spepublications.onlinelibrary.wiley.com/doi/10.1002/pc.70332, Wiley Online Library on [26/08/2025]. See the Terms and Conditions (https://onlinelibrary.wiley.com/terms-and-conditions) on Wiley Online Library for rules of use; OA articles are governed by the applicable Creative Commons License

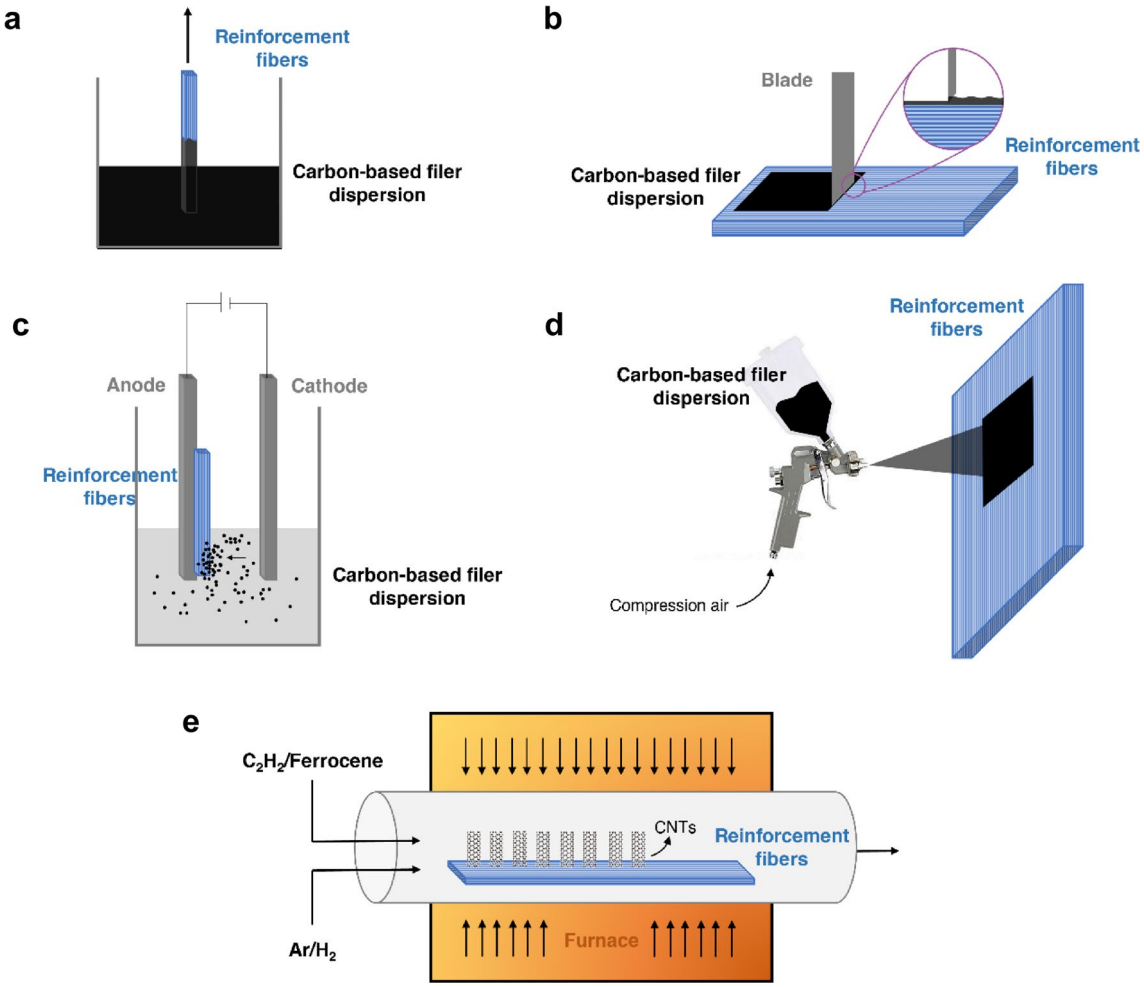


FIGURE 6 | Schematic representation of the coating techniques for GFRPs: (a) dip-coating, (b) doctor blade coating, (c) electrophoretic deposition (EPD), (d) spray coating, and (e) chemical vapor deposition (CVD).

especially the first hydrolysis step, where the consumption of alkoxysilanes is normally easy to monitor, since it is assumed to be an elementary reaction. The first hydrolysis step also controls the overall reaction, because it is the slowest step [156]. Hydrolysis and condensation have their own kinetic parameters, and each step has indefinite numbers of reactions close to or at equilibrium, due to polymerization and de-polymerization processes. Mechanisms and rates of the reactions are remarkably influenced by several parameters, such as acidic, neutral, and alkaline media, as well as the presence of catalysts and the water/silane molar ratio [157].

Specifically, the pH of the silane solution as well as the presence of surface micro-heterogeneities in GF affect the surface potential of the substrate, leading to a variation in the orientation of the adsorbed silane layers [158]. Moreover, the drying conditions (i.e., temperature and duration) used on the silane-treated GF also influence the extent of siloxane bond formation, both between neighboring silane molecules and between the silanes and the substrate surface [159].

From a thermodynamic perspective, the binding of silane molecules results in a loss of conformational freedom in the silane tail, leading to an entropy cost for the system. However, this entropy loss can be offset by the enthalpic gain from ligand binding to the surface, ultimately contributing to the overall stabilization of the system [160, 161].

After the modification of the GF, the bonding of the siloxane film and the polymer matrix occurs via a combination of interpenetration and chemical reactions through hydrogen bonds, which lead to the generation of polymer/siloxane/glass "interphase" (Figure 7).

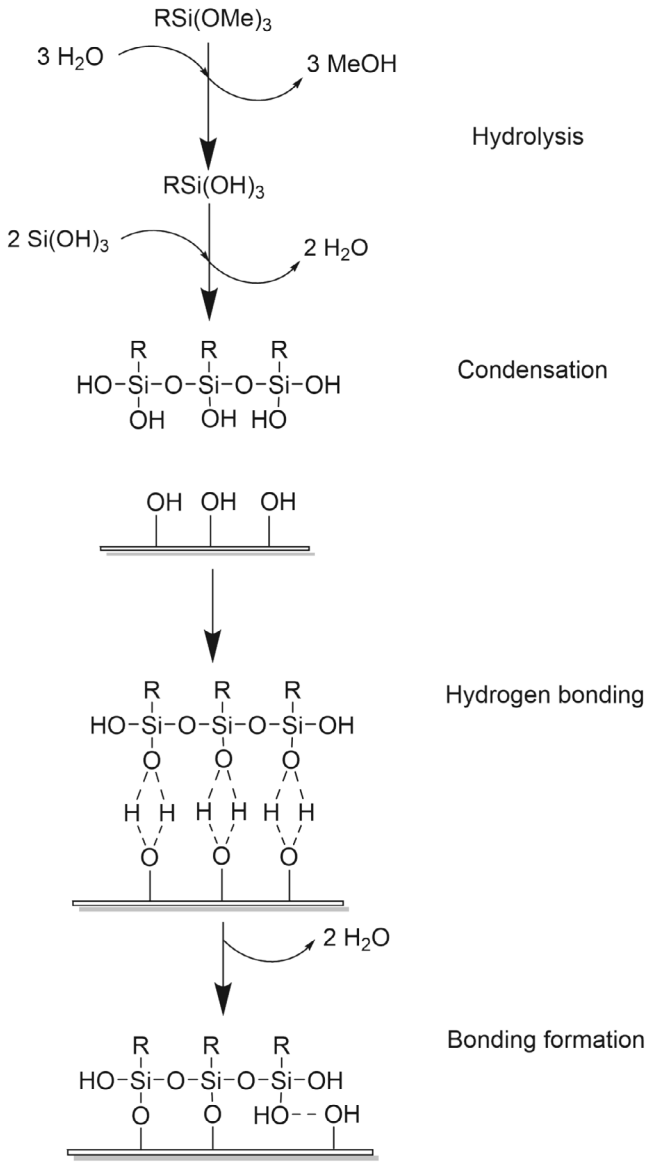
According to the Plueddemann model [158], this region is described as a monomolecular layer of hydrogen bonds that connect a rigid polymer and the siloxane network (see highlight in Figure 7).

Three main factors influence this process:

- The chemical reactivity between the functional groups of the coupling agents and those of the matrix to form covalent bonds.
- The generation of primary or secondary chemical bonds at the glass interface.
- The diffusion of the polymer chains into the siloxane "interphase" film to develop a rigid, water-resistant interpenetrating polymer network between the GF surface and the bulk matrix (diffuse interphase).

15480569, 0, Downloaded from https://4spepublications.onlinelibrary.wiley.com/doi/10.1002/pc.70332, Wiley Online Library on [26/08/2025]. See the Terms and Conditions (https://onlinelibrary.wiley.com/terms-and-conditions) on Wiley Online Library for rules of use; OA articles are governed by the applicable Creative Commons License

The mechanical and chemical properties of the "interphase" play a crucial role in determining the durability of the composite material. The breaking and reforming of hydrogen bonds minimize stress concentrations at the interface between the GF and matrix while maintaining molecular contact beneath the rigid siloxane network [158]. However, temperature variations, moisture ingression, sunlight exposure, oxidation, microbiologic attack, and other environmental elements may lead to significant alterations of the interphase region, with negative fallouts on the final performance of the composite structures, especially in their long-term utilization [6].



SCHEME 1 | Hydrolysis and condensation of alkoxysilane on the glass fiber surface.

In detail, when water penetrates the interphase, it hydrates the Si—O—Si and Si—O—C bonds. Concurrently, competing self-condensation reactions of silanol groups can generate various oligomeric species within the crosslinked siloxane layer [153]. The infiltration of absorbed water molecules occurs along the fiber/matrix interface and in the presence of cracks or microscopic voids via capillary action and diffusion, giving rise to several damage mechanisms like matrix cracking, fiber–matrix debonding, and corrosion of fibers (especially in the case of glass fiber) [162–164]. These, in turn, promote a substantial reduction in modulus, strength, and ultimate strain [165]. For instance, Birger et al. reported that graphite fabric/epoxy composites subjected to hydrothermal aging in boiling water for a relatively short time (46 h) demonstrated substantial reductions in both shear and tensile strengths [166]. This degradation is primarily attributed to the breakdown of fiber–matrix interfacial adhesion, resulting in exposed fibers and the formation of significant matrix voids.

Temperature-induced damage has been shown to further accelerate moisture diffusion in composite materials [167]. Several studies have investigated the behavior of composites under hygrothermal conditions under mechanical loading. Ray et al. reported that symmetric and anti-symmetric GFRP laminates exposed to a 98% relative humidity environment for 2000 h undergo flexural stiffness reductions of 54% and 27%, respectively [168]. Also, hygrothermal degradation of unidirectional glass fiber/epoxy composites has been characterized through moisture sorption/desorption experiments and dynamic mechanical thermal analysis (DMTA). Furthermore, both static and fatigue strength reductions in carbon fiber/epoxy composites under hygrothermal conditioning have been retrieved [168].

These studies point out the delicate action of the silanes at the GF/matrix interface in influencing the bond strength and the durability of GFRPs. In addition to this role, the functional groups

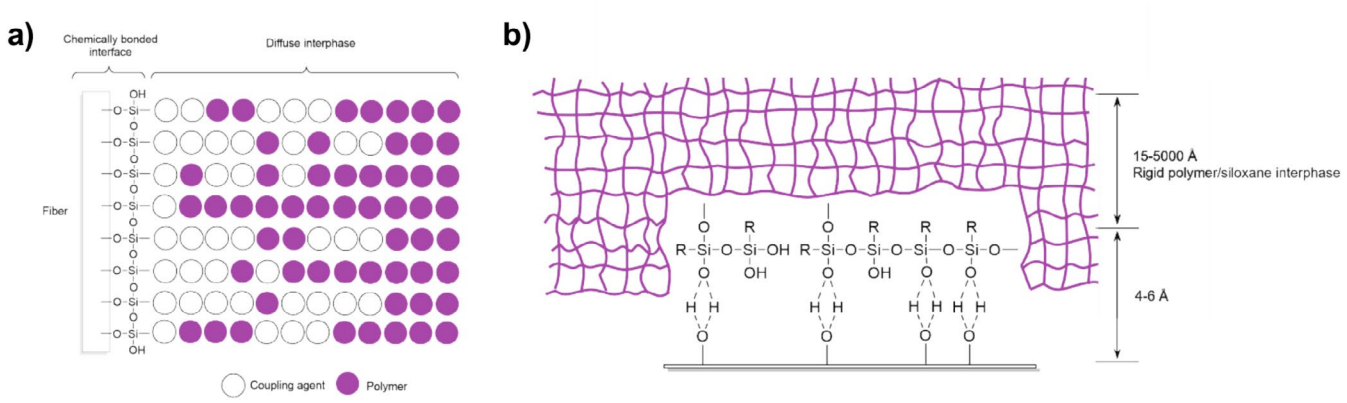


FIGURE 7 | Graphic representations of (a) bonding of siloxane and polymer chains; (b) polymer/siloxane/glass fiber interphase.

15480569, 0, Downloaded from https://4spepublications.onlinelibrary.wiley.com/doi/10.1002/pc.70332, Wiley Online Library on [26/08/2025]. See the Terms and Conditions (https://onlinelibrary.wiley.com/terms-and-conditions) on Wiley Online Library for rules of use; OA articles are governed by the applicable Creative Commons License

of organosilane coupling agents represent a "bridge" for anchoring carbonaceous systems, such as CNTs and graphene-based materials. CNTs and graphene can form covalent or van der Waals bonds with both GF and the polymer matrix. Moreover, the surface functionalization of these nanomaterials with reactive groups may further promote the formation of covalent bonds with the matrix, thereby improving interfacial adhesion and avoiding the potential leaching of the conductive coating when the fabrics are introduced into the polymer matrix.

While several reports in the literature describe the deposition of MWCNTs via chemical bonding onto the surface of carbon fibers, exploring their surface morphology and the enhancement of interfacial strength [169–173] far fewer papers deal with an effective chemical approach for grafting MWCNTs onto the surface of GF. A convincing approach was proposed by Tzounis et al. [174], who functionalized single GF with aminopropyltriethoxysilane, yielding amine surface functionalities able to covalently interact by amidation reaction with acyl chloride-modified MWCNTs (MWCNT-COCl) and resulting in the formation of GF-MWCNTs. To highlight the role of covalent bonding, the same GF were also immersed in a solution of carboxylated MWCNTs (MWCNT-COOH), just leading to the physical adsorption of nanotubes on the fiber surface through hydrogen bonds or zwitterionic interactions (GF-ad-MWCNTs). The nature of the bonding significantly impacted the electrical properties of the hybrid GF, composite interfacial microstructures, and interfacial adhesion strength. Both modification strategies lead to the generation of conductive filaments; however, GF-MWCNTs demonstrated an order of magnitude higher electrical conductivity due to the uniform coating of the MWCNT surface as well as greater durability of the grafted MWCNTs, which remained attached to the fiber surface after being embedded in the epoxy matrix. This remarkable stability was linked to the highest interfacial adhesion strength observed in the GF-g-CNT microcomposites, as determined by single-fiber pull-out tests (see Figure 8), which revealed an increase of ~48% in the apparent interfacial shear strength (IFSS) compared to that of the reference silanized GFs.

A similar approach was exploited by Eskizeybek et al. [175] to prepare amide-functionalized glass fabrics using (3-Aminopropyl)triethoxysilane (APTES) which was then reacted with carboxylic acid-functionalized CNTs. This process resulted in the formation of covalent amide linkages between the carboxylic acid-functionalized CNTs and the amino groups on the APTES-treated glass fabrics. Multi-scale composites based on plain woven glass fabric (PWGF)/CNT/epoxy were then fabricated using vacuum-assisted resin infusion molding. Tensile and flexural tests were conducted to evaluate the impact of grafting CNTs onto the PWGF surface on the mechanical properties of the resulting multi-scale composites. In particular, pull-out tests revealed that CNTs remained on the fiber surface after failure. This observation can be directly attributed to the strong covalent interactions between the CNTs and glass fiber, which hold them strictly on the surface during pull-out.

Another interesting and simple strategy to graft CNTs onto GF was suggested more recently by Fang et al. [176, 177]. They improved the interfacial properties between glass fibers and polyamide 6 (PA) and isotactic polypropylene (iPP) matrices by introducing polyethyleneimine (PEI) functionalized carboxylic MWCNTs onto the surface of glass fibers through aqueous solution mixing (Figure 9a). PEI-CNT formed a compact and homogeneous network structure on the glass fiber surface via a grafting reaction to introduce plentiful active functional groups and gain surface roughness. The network structure is employed to enhance mechanical interlocking at the interface, improve the wettability of glass fibers, and easily form hydrogen bonds with PA6. In particular, the enhanced interfacial adhesion was proven by interfacial shear strength (IFSS), which increased by 39.5% compared to that of iPP mixed with raw GF. The protocol was then extended to GO, resulting in enhanced strength and toughness of the interfacial region between the GFs and polymer matrix (Figure 9b).

Similarly to what has been done for CNTs, Chen et al. [178] covalently grafted GO units on GF surface through an amidation reaction between the carboxylic groups of GO and the amino groups of APTES molecules anchored to the fiber surface (Figure 10a).

The behavior of the obtained hybrid fibers (GO-g-GF) was compared with that of GF coated with GO obtained via the electrostatic assembly strategy (GO-c-GF). The short beam shear method was then used to evaluate the ILSS of the epoxy

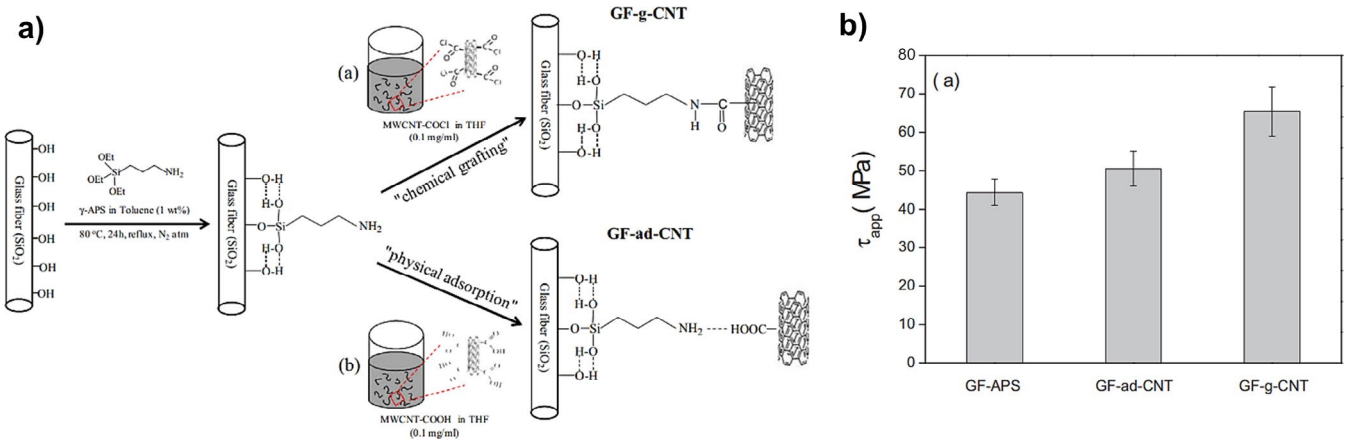


FIGURE 8 | (a) Protocol for the preparation of physically adsorbed and chemically grafted MWCNTs on GF; (b) IFSS obtained with single-fiber pull-out tests. Reproduced with permission from [174].

15480569, 0, Downloaded from https://4spepublications.onlinelibrary.wiley.com/doi/10.1002/pc.70332, Wiley Online Library on [26/08/2025]. See the Terms and Conditions (https://onlinelibrary.wiley.com/terms-and-conditions) on Wiley Online Library for rules of use; OA articles are governed by the applicable Creative Commons License

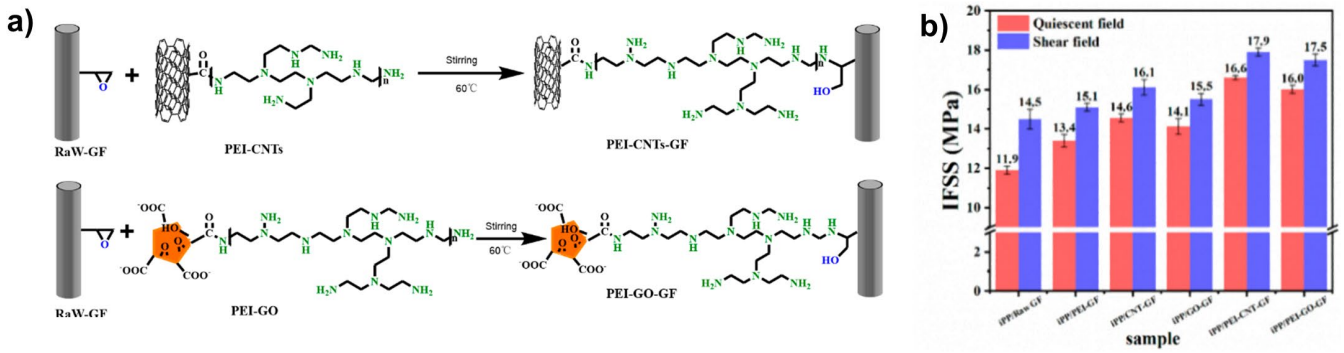


FIGURE 9 | (a) Protocol for the synthesis of PEI-CNT and PEI-GO on the GF surface; (b) IFSS of various iPP/GF micro-composites under quiescent and shear fields, respectively. Reproduced with permission from [176].

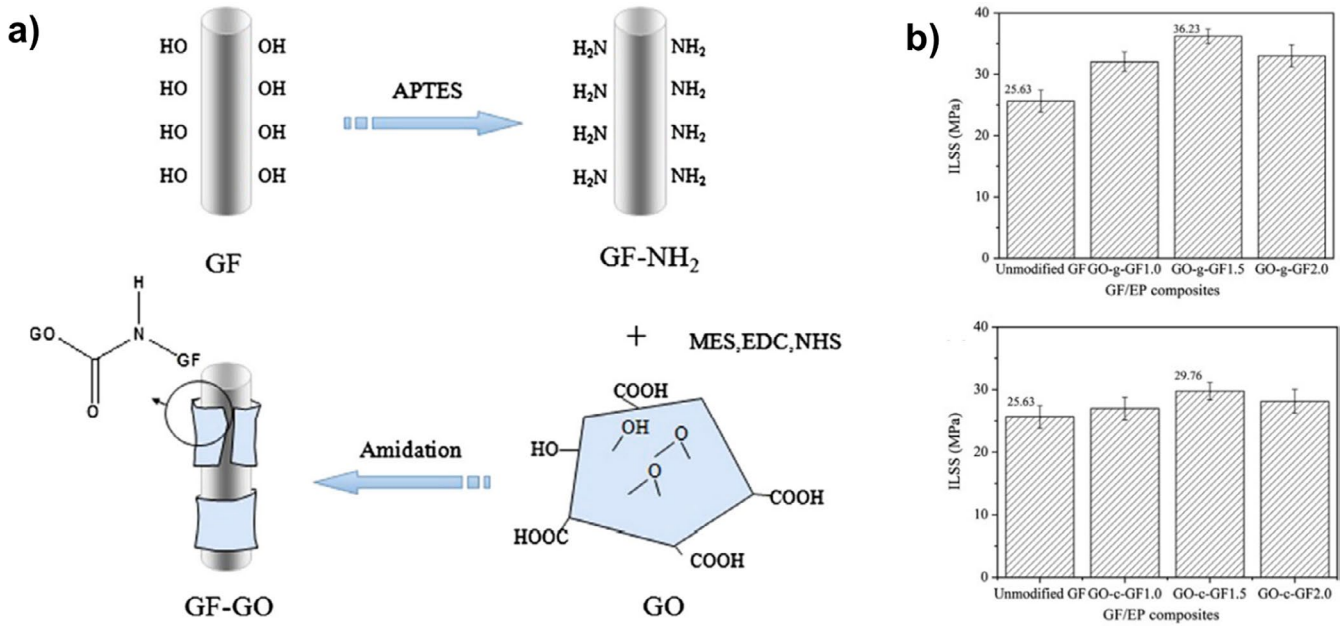


FIGURE 10 | (a) Protocol for the preparation of GO-g-GF; (b) interlaminar shear strength of GF/epoxy composites. Reproduced with permission from [178].

composites prepared by enclosing GO-g-GF and GO-c-GF. The results revealed that the concentration of the GO solutions used for both grafting and electrostatic adsorption affected the interfacial properties of the materials. In particular, GO-g-GF systems reached higher ILSS values than those of the bare GF and GO-c-GF prepared with a comparable amount of GO (Figure 10b). These outcomes indicate a remarkable increase in the interfacial adhesion, which can be ascribed to an enhanced mechanical interlocking between the GF surface and matrix as a result of the increased roughness provided by GO grafting.

Hua et al. [179] employed the same mechanism to graft a mixture of CNTs and GO onto GF to create GO/CNT-modified GF. The two-dimensional GO and one-dimensional CNTs were entangled, with GO serving as the encapsulating component and CNTs acting as the anchoring element. This combination synergistically improved the properties of the GF composite. The interfacial bond strength of the GO/CNT hybrid coating was 128% higher than the value predicted by the rule of mixtures, based on the results of the individual GO and CNT coatings, highlighting the significant cooperative effect of the hybrid coating in enhancing the interfacial bond strength.

In summary, the chemical grafting of CNTs and graphene can be a viable route to significantly enhance the interfacial properties of GFRPs, thus contributing not only to the electrical conductivity, which is essential for SHM, but also imparting superior mechanical performance and improved durability to the composites.

Since they serve as critical feedback for optimizing the process and identifying the most effective fiber surface modifications, a brief overview of the main micro (e.g., fiber pull-out, fiber push-out, and micro-droplet tests) and macro-scale mechanical tests (e.g., short beam shear tests) characterizing the fiber/matrix interfacial bonding properties is provided in the next section. Finally, the principal electrical testing methods, which are essential tools for the precise analysis of self-sensing efficacy, are concisely described.

15480569, 0, Downloaded from https://4spepublications.onlinelibrary.wiley.com/doi/10.1002/pc.70332, Wiley Online Library on [26/08/2025]. See the Terms and Conditions (https://onlinelibrary.wiley.com/terms-and-conditions) on Wiley Online Library for rules of use; OA articles are governed by the applicable Creative Commons License

5 | GF/Matrix Interfacial Characterization Tests

5.1 | Preliminary Remarks

Numerous techniques have been developed to characterize the fiber/matrix interfacial strength, targeting either the individual fiber (micro-scale testing) or the full laminate (macro-scale testing), especially in the field of continuous fiber composites. Nonetheless, the discussion regarding which method is the most accurate and reliable continues [180].

At the fiber level, relevant methods include fiber microdebonding, single fiber pull-out, single fiber push-out, and single-fiber fragmentation [181]. These techniques are advantageous as they isolate the fiber–matrix interaction, enabling precise measurement of interfacial properties. Although microdebonding and fiber pull-out are adaptable to various fiber-matrix combinations, they are constrained by their small scale, potential unrepresentativeness of specimens, and challenges in accurately evaluating droplet geometry and size [180]. The single-fiber fragmentation test offers valuable insights into the failure process, especially in transparent matrices, but it necessitates specific matrix properties. The push-out test facilitates in situ measurement within the actual composite environment, because the test can be performed on a small portion of an actual laminate and preparing an ad hoc model composite is not necessary, though it poses difficulties in observing the failure mode [182].

At the laminate level, techniques such as short-beam shear (SBS), Iosipescu shear, and [±45°] tensile tests provide a more comprehensive evaluation of interfacial properties within the composite structure, so in a more realistic environment [183]. However, they may be affected by factors beyond the fiber-matrix interface. The variety of these techniques, each with its own set of strengths and limitations, highlights the complexity of characterizing fiber-matrix adhesion, indicating that a thorough approach employing multiple methods may offer the most robust understanding of interfacial properties in continuous fiber composites [184].

5.2 | Micromechanical Test

The most common micro mechanical testing methods used to assess the fiber-matrix interface of fiber reinforced polymers include the fiber fragmentation test, the droplet strip-off (microbond) test, the single fiber pull-out test, and the single fiber pushout test. Each of these methods generates predominant shear stress at the interface, allowing for the calculation of the interfacial shear strength (IFSS).

In the fiber fragmentation test (Figure 11a), a single fiber is embedded within a bone-shaped tensile test sample made of the polymer matrix material. During the stretching of the sample, longitudinal deformation induces shear stresses along the embedded fiber, resulting in axial stresses inside the fiber. Thus, the fiber fragments into segments. The length distribution of these segments provides valuable information regarding the "critical lengt," which is defined as the length at which the transferred stress vis the interface is sufficient to exceed the fiber's strength. This test assumes uniform shear stress along the segments, neglecting stress concentrations at the edges of the segments, as well as partial debonding and stress transfer due to friction. The test is applicable to transparent or at least opaque polymers that exhibit a higher elongation-to-break than the tested fiber. This poses challenges for investigating matrix polymers such as epoxy or PEEK. Additionally, the evaluation requires assumptions regarding the strength distribution of the embedded fiber [185–189].

The droplet strip-off test, also referred to as the microbond test, involves the application of small droplets of the matrix polymer onto a single fiber (Figure 11b). For improved handling, the fiber is slightly pre-stretched and fixed in a vertical position. After solidification of the droplets, a pair of knife edges is employed to strip a droplet along the fiber. The resulting force must overcome a combination of the resistance of adhesion and friction. The droplet strip-off method offers advantages such as relatively simple preparation and minimal material requirements. However, the use of knife edges, in conjunction with the conical shape of the droplets near the fiber, may introduce a complex stress field that could alter the results [190–193].

A variant of the droplet strip-off test is the single fiber pull-out test (Figure 11c). In this method, a single reinforcing fiber is partially immersed in a liquid droplet for a specified embedding length. The droplet is typically placed on a fixed support that can be heated to melt a thermoplastic polymer or cure a thermoset. After the matrix solidifies, the free end of the embedded fiber is attached to a moving stage equipped with a force

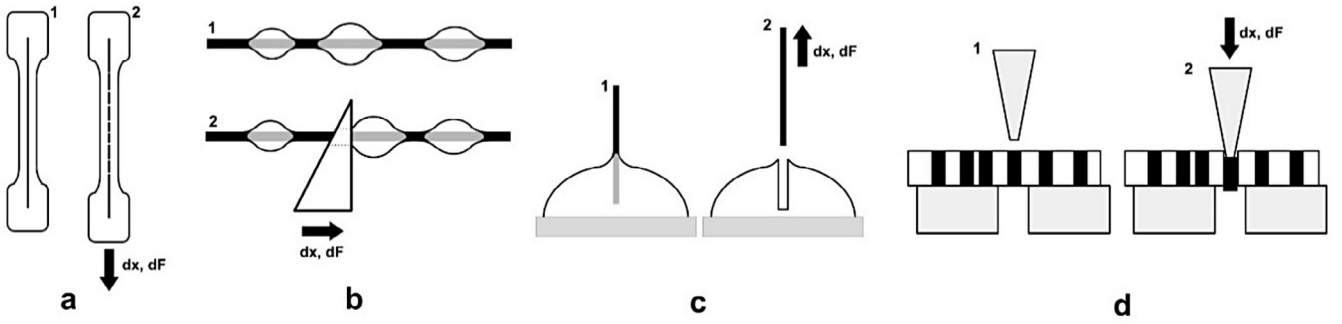


FIGURE 11 | Principles of common micromechanical tests for assessing the fiber-matrix interface: (a) fiber fragmentation test, (b) droplet strip-off test, (c) single fiber pullout test, and (d) fiber pushout test.

15480569, 0, Downloaded from https://4spepublications.onlinelibrary.wiley.com/doi/10.1002/pc.70332, Wiley Online Library on [26/08/2025]. See the Terms and Conditions (https://onlinelibrary.wiley.com/terms-and-conditions) on Wiley Online Library for rules of use; OA articles are governed by the applicable Creative Commons License

transducer and is gradually pulled out of the droplet. The single fiber pullout test provides comprehensive information regarding the fiber-matrix contact and the applied force-displacement function. Various fiber-matrix combinations can be tested if the fiber is stiff enough and the matrix material has a low viscosity enabling the preparation [194–197].

The formerly described methods are primarily designed for testing samples composed of single fibers and a limited amount of matrix under controlled laboratory conditions. Consequently, these samples may not accurately represent the conditions experienced by real-life technical components, which undergo a processing history, mechanical stresses during their application, and environmental influences such as temperature fluctuations, humidity, and radiation.

The single fiber pushout test (Figure 11d) is applicable to technical real-life fiber reinforced composites. For preparing test samples, a thin slice is prepared such that the fibers are oriented normal to the slice surface. Care must be taken to ensure that the slice is sufficiently thin to facilitate pushout without causing fiber breakage under pressure. The slice is positioned over a small groove, allowing the pushed fiber to move freely in air rather than against a solid resistance. For the test, a flat cone punch, matching the fiber diameter, is precisely lowered over a single fiber segment to push it out while recording force and displacement. The disadvantages are the time-consuming preparation process for the thin slices and the complex test device. On the other hand, a single preparation can provide hundreds of fiber segments ready for testing [180, 198–201].

5.3 | Macro Mechanical Tests

Macro-mechanical testing methods offer valuable insights into the interfacial properties of fiber-reinforced composites by evaluating the entire laminate structure. These tests provide a more realistic assessment of interfacial strength in actual composite applications compared to micro-scale tests. These tests are designed to induce shear stress in the laminate, which often causes a failure of the interfacial/interlaminar region. If the failure is adhesive, that is, deriving from a detachment of the matrix from the fiber, and not cohesive, that is, deriving from the rupture of either the matrix or the fibers, then the tests can be directly used to measure the interfacial shear strength. Otherwise, these tests provide just an indirect indication of the fiber/matrix adhesion [181].

Three prominent macro-mechanical tests widely used for characterizing interlaminar, or in-plane shear properties are the Iosipescu shear test, the ±45° tensile test, and the short beam shear test, which are described in the next sections; although other tests exist such as rail shear or the asymmetric four-point bending (AFPB). It is worth mentioning that the evaluation of the fiber/matrix adhesion can also be performed via the 90° tensile test, where the fibers are oriented perpendicular to the applied load. In this case, if the fracture is adhesive, the maximum load can be used to calculate the interfacial normal stress [202].

5.3.1 | Iosipescu Shear Test

The Iosipescu shear test, standardized as ASTM D5379/D5379M, is primarily designed for measuring in-plane shear properties of materials, such as shear modulus and strength, and utilizes a specialized fixture to induce a state of pure shear in a notched specimen. Specimens are typically rectangular, measuring 76.2 mm × 19.1 mm × thickness (minimum 2.5 mm), with two 90° V-notches at the midpoint of the longitudinal edges, creating a reduced cross-section area where shear failure is expected to occur (Figure 12a).

The test employs a specialized fixture with two halves: one stationary and one movable (Figure 12b). The specimen is positioned in the fixture such that the notched section is aligned between the loading points. During testing, the fixture applies opposing forces, creating a pure shear condition in the region between the notches. The test is conducted at a constant displacement rate of 2 mm/min until failure occurs. Load and displacement are recorded throughout the test, and strain gauges oriented at ±45° to the loading direction can be attached to the specimen center to measure shear strain.

The shear strength (τ) is calculated as $\tau = P/A$, where P is the maximum applied load (N), and A is the cross-sectional area between the notches (mm^2). The test provides detailed information on shear modulus, ultimate shear strength, and shear stress–strain behavior [202]. If the fracture is adhesive, then the calculated shear strength can be used to evaluate the (interlaminar) fiber/matrix interfacial strength.

5.3.2 | ±45° Tensile Test

The ±45° tensile test, standardized under ASTM D3518/D3518M, measures the in-plane shear properties of composite laminates using a symmetric laminate with fibers oriented at ±45° to the loading direction. Specimen preparation follows ASTM D3039 guidelines with typical dimensions of 250 mm × 25 mm × thickness, though the lamination sequence specifically consists of an even number of plies with alternating +45° and −45° orientations relative to the longitudinal axis (Figure 12c).

The specimen is mounted in a universal testing machine using appropriate grips, with tabs often bonded to the specimen ends to prevent grip-induced damage. The test is conducted at a constant crosshead speed; both longitudinal and transverse strains are measured using strain gauges or extensometers. The applied tensile load generates shear stresses in the principal material directions (along and perpendicular to the fibers) [203].

The in-plane shear stress (τ_{12}) is calculated as $\tau_{12} = \sigma_x/2$, where σ_x is the applied axial stress (MPa). The in-plane shear strain (γ_{12}) is determined as $\gamma_{12} = \varepsilon_x - \varepsilon_\gamma$, where ε_x is the longitudinal strain and ε_γ is the transverse strain [181]. The in-plane shear modulus G_{12} is calculated as the slope of the shear stress–strain curve at low strain levels (typically between 0.1% and 0.5% shear strain), as $G_{12} = \Delta\tau_{12}/\Delta\gamma_{12}$. This test provides valuable information about the fiber-matrix interface quality, as shear loading predominantly stresses this interface and the failure mechanism is often linked to interfacial failure.

15480569, 0, Downloaded from https://4spepublications.onlinelibrary.wiley.com/doi/10.1002/pc.70332, Wiley Online Library on [26/08/2025]. See the Terms and Conditions (https://onlinelibrary.wiley.com/terms-and-conditions) on Wiley Online Library for rules of use; OA articles are governed by the applicable Creative Commons License

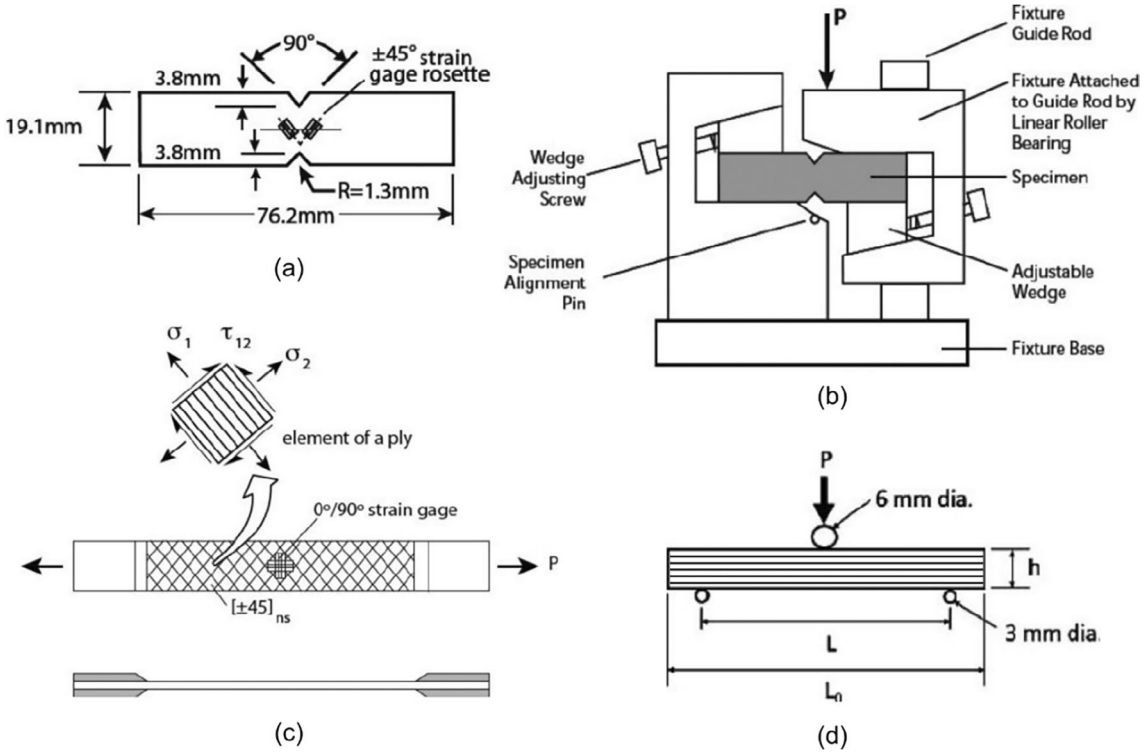


FIGURE 12 | (a) Specimen for iosipescu test; (b) setup for Iosipescu test; (c) specimen and stress state for ±45° tensile test; (d) specimen and test setup for short beam shear test. Adapted with permission from [203].

5.3.3 | Short Beam Shear Test

The short beam shear (SBS) test, standardized as ASTM D2344/D2344M, is the most widely used macro-mechanical test for assessing interlaminar shear strength due to its simplicity and efficiency. The test utilizes a three-point bending configuration with a significantly reduced span-to-thickness ratio (typically 4:1 to 5:1, compared to 16:1 or higher for flexural tests) to promote interlaminar shear failure rather than tensile or compressive failure (Figure 12d).

Specimen preparation is straightforward, requiring simply a rectangular beam typically measuring 24 mm × 8 mm × thickness, with the thickness dependent on the material being tested (usually between 2 and 6 mm). For unidirectional composites, fibers are oriented along the longitudinal direction of the beam. The specimen is placed on two supporting rollers, and a loading nose applies force at the midpoint.

The test is conducted at a constant crosshead speed until failure occurs. Load–displacement data is recorded throughout the test. The short beam strength, corresponding to the interlaminar shear strength if the failure is in the interlaminar region, as often occurs, is calculated as $\mathrm{ILSS} = 0.75 \times P/(w \times t)$, where P is the maximum load observed (N), w is the specimen width (mm), and t is the specimen thickness (mm) [181]. The factor 0.75 is derived from beam theory analysis for the maximum shear stress in a beam with a rectangular cross-section. Again, if the failure occurs due to the detachment of the fibers from the matrix, the ILSS gives an indication of the interfacial adhesion.

While the SBS test is widely used due to its simplicity, it should be noted that the state of stress is not pure shear, as flexural stresses are also present. Additionally, stress concentrations at loading points can influence results. Despite these limitations, the test provides a practical and efficient method for comparative assessment of interlaminar shear strength, particularly useful for quality control and process optimization [203].

Table 2 reports a review of the recent progress in the ILSS improvement of GFRPs after the incorporation of conductive nanofillers through different modification methods. In general, CNTs and graphene oxide significantly enhance the interfacial properties of epoxy composites due to their increased surface area, improved chemical bonding, and effective stress transfer.

Although referring to different systems, the available results support the validity of the chemical grafting in providing a remarkable improvement of the ILSS of GFRPs.

6 | Electrical Test for the SHM Assessment and Damage Analysis

6.1 | Preliminary Remarks

Electrical health monitoring exploits anisotropic conductivity in Carbon Fiber Reinforced Polymers (CFRPs) and nanomodified GFRPs to detect and quantify various damage modes. It is well established that the initial phases of static and fatigue loading in multidirectional laminates composed of unidirectional (UD)

15480569, 0, Downloaded from https://4spepublications.onlinelibrary.wiley.com/doi/10.1002/pc.70332, Wiley Online Library on [26/08/2025]. See the Terms and Conditions (https://onlinelibrary.wiley.com/terms-and-conditions) on Wiley Online Library for rules of use; OA articles are governed by the applicable Creative Commons License

TABLE 2 | A summary of ILSS enhancement in GFRPs with CNTs and GO.

Material (filler/fiber/matrix)	Modification method	Improvement ILSS (%)	References
CNTs-NH_2/glass/epoxy	Matrix modification via mixing	20	[204]
MWCNTs/glass/epoxy	Fiber modification via spray coating	26.7	[205]
CNTs/glass/epoxy	Fiber modification via grafting with CVD	23.9	[74]
MWCNTs/glass/epoxy	Fiber modification via dip-coating	25.2	[206]
CNTs/glass/epoxy	Fiber modification via EPD	42	[207]
CNTs/glass/epoxy	Fiber modification via chemical grafting	43.1	[208]
CNTs/glass/epoxy	Fiber modification via chemical grafting	21.6	[209]
GO/glass/epoxy	Matrix modification via mixing	32.7	[210]
rGO/glass/epoxy	Fiber modification via spray coating	10.7	[152]
GO/glass/epoxy	Fiber modification via EPD	15	[136]
GO/glass/epoxy	Fiber modification via chemical grafting	41.2	[178]

plies are marked by the initiation and growth of cracks within the off-axis plies. The transverse crack density increases progressively either with the applied static load level or with the number of loading cycles. This leads to a degradation of the overall elastic properties and facilitates the onset of additional damage mechanisms such as delamination and fiber breakage.

Within this scenario, it is evident that reliable methods for the health monitoring of composite materials are essential, and among the possible strategies to be used, the Electrical Health monitoring offers significant advantages, being a cheap and sensorless method. The concept of electrical health monitoring (EHM) via carbon-fiber conductivity traces back to Schulte and Baron [211], who first correlated load-dependent conductivity with strain and fiber damage.

Several subsequent works further extended Schulte's pioneering investigations; scrutinized the monitoring of delamination and matrix cracking under various loads [212–222]. In CNT-doped epoxy nanocomposites, propagating cracks disrupt conductive pathways, increasing resistivity proportionally to crack length (see Ref. [223] for more details).

Differently, in CFRPs, high along-fiber conductivity yields excellent sensitivity to fiber failure and delamination; for example, in Ref. [224] up to 30% resistance increase was noted in DCB tests. Differently, matrix cracks evoke modest changes (~0.4%) in the electrical resistance of composite specimens [214, 216], even if incorporating conductive nanoparticles could improve transverse conductivity and overall damage sensitivity [225].

In the case of insulating glass fibers, CNT or carbon-black doped matrices form 3D conductive networks that detect matrix cracks and delamination detection [204, 226–238]; though dispersion and viscosity pose manufacturing challenges. CNT coatings applied via CVD, EPD, dip-coating, or sizing enhance conductivity by orders of magnitude compared to bulk doping [174, 235, 239–242] and allow to effectively sense fiber breakage and delamination [243, 244].

Within this context, it is also worth mentioning that reliable EHM also demands proper electrode techniques (four-probe methods are usually used to minimize contact resistances) and meticulous surface preparation (such as superficial resin removal in CFRPs) [224, 245–255].

6.2 | Electrical Health Monitoring of CFRPs

Focusing the attention on Carbon Fiber Reinforced Polymers, early studies confirmed that off-axis matrix cracks incrementally raise the composite's electrical bulk resistance [216, 256–261] (Figure 13).

For example, in stepped tensile experiments on [0/90/0] laminates, load–unload sequences produced increasing residual $\Delta R/R_0$ correlated with rising crack density [216]; during these tests, optical replica analysis showed crack initiation at ~0.3% strain, matching the onset of $\Delta R/R_0$ growth, though peak resistance changes remained below 0.5% due to dominant in-plane conduction paths [216].

Delamination is another important damage event in composite materials, interrupting through-the-thickness current paths sharply. Initial demonstrations on [0/90] cross-ply specimens by Wang and Chung [50] and Irving and Thiagarajan [256] showed irreversible resistance jumps concurrent with delamination propagation [213, 262–265].

Eventually, fiber breakage, often triggered where transverse cracks intersect load-bearing plies or where fibers bridge cracks, significantly alters the conductive network [212]. Saw-cut tests on uncycled [0] laminates verified that severing fibers proportionally increases resistivity, moderated by inter-fiber contacts [211, 221]. During static tension, resistivity varies linearly with strain (as $R = \rho L/A$) until ~0.7% strain, where micro-failures emerge; then exhibit stepwise jumps beyond ~1.2% strain corresponding to catastrophic fiber fracture [211].

15480569, 0, Downloaded from https://4spepublications.onlinelibrary.wiley.com/doi/10.1002/pc.70332, Wiley Online Library on [26/08/2025]. See the Terms and Conditions (https://onlinelibrary.wiley.com/terms-and-conditions) on Wiley Online Library for rules of use; OA articles are governed by the applicable Creative Commons License

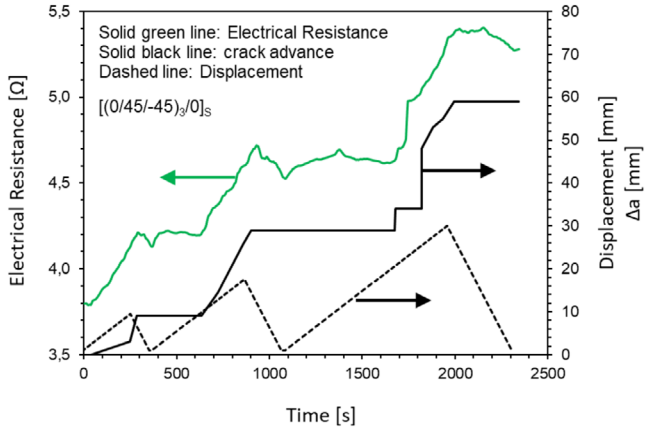


FIGURE 13 | Resistance, displacement, and delamination length versus time during Mode-I DCB testing on CFRP. Adapted with permission from [262].

6.3 | Electrical Health Monitoring of Nanomodified GFRPs

As mentioned in the previous sections, in the case of Glass Fiber Reinforced Polymers, the conductivity properties needed to carry out electrical HM are obtained either by doping the polymer matrix or the glass fibers surface (CNT fiber coatings).

In the case of CNT-doped matrix GF laminates, microcracking yields gradual resistance rise, while delamination triggers abrupt jumps [234, 235]. Stepped tensile tests on CNT/epoxy glass laminates detected irreversible $\Delta R/R_0$ of ~0.02% for residual strains as low as 0.05% [234]. Comparative tests demonstrate that matrix nanomodification achieves greater $\Delta R/R_0$ sensitivity than fiber coating [266, 267].

6.4 | Brief Hints on Models for Resistivity Prediction in Nanomodified Epoxy Laminates

Based on the aforementioned studies, the methodology relying on electrical measurements appears to be a promising approach for detecting the initiation and progression of cracks in both CFRPs and GFRPs. However, the successful application of these methods for health monitoring of composite parts requires the development of models that can reliably predict the damage state based on resistance measurements.

In this perspective, a deeper understanding of the key material and geometric parameters influencing the phenomenon, as well as accurate quantification of their effects, is needed. Among the limited numbers of analytical methods reported in the literature, a relevant example is the orthotropic electric potential function approach developed by Todoroki [268], which is based on a formal analogy with the field equations governing fluid flow. Initially formulated for an infinite plate, this method was later employed by the same author to investigate changes in electrical voltage caused by delamination in CFRP [269–271].

A completely different analytical method to predict the electrical response of a typical CFRP composite in an epoxy matrix nanomodified with CNTs and with a delamination was recently proposed by Zappalorto et al. [224]. This strategy involves the discretization of the laminate through its thickness into a definite number of "fictitious" sublayers, within which the electrical potential is approximated using a polynomial function. By applying the fundamental equations governing the electric field and incorporating appropriate boundary conditions, analytical expressions for the current densities can be derived. This, in turn, enables the analytical evaluation of the electric potential drop between any two arbitrary points in the delaminated laminate. The method was applied to a Double Cantilever Beam (DCB) specimen to calculate the electric potential of a point on the laminate surface and to evaluate its modification along the delamination length. The accuracy of the theoretical predictions was validated through several finite element analyses, which demonstrated excellent agreement with the experimental results.

The same strategy was extended by the authors to generic multidirectional laminates with delamination cracks, including generic off-axis angles for all the plies [262]. The analytical solution was initially validated using results from a series of Finite Element (FE) analyses conducted on multidirectional laminates with varying delamination lengths. The effects of laminate layup and material electrical properties were investigated, revealing that multidirectional laminates exhibit greater sensitivity to delamination compared to unidirectional ones. An experimental campaign was successively carried out on both unidirectional and multidirectional DCB specimens, measuring the delamination length and the electrical resistance change, revealing a clear correlation between these two properties. The experimental results were subsequently compared with the analytical predictions, showing very good agreement, demonstrating the effectiveness of electrical measurements for monitoring delamination, in particular in CNT-modified glass fiber-reinforced laminates [242]. More recently, a general analytical model for correlating the bond line crack length to the joint electrical response was developed and applied also on CNT-modified GFRP laminates and CFRP [272]. The model was validated through FE analyses and experimental tests, which revealed a satisfactory accuracy level on single lap joints made of Al adherends and a conductive epoxy adhesive. Conversely, a lower sensitivity to the damage presence was attained for carbon/epoxy composites. This was attributed to the non-ideal insulating properties of the crack faces, caused by fiber bridging and crack propagation occurring both along the interface and within the adherends. To address this, the model was refined to include a residual crack face conductivity, represented by a single parameter (φ). This modification allowed the formulation of a revised procedure for implementing the EHM in laminate bonded joints. The proposed methodology was subsequently validated against a benchmark case, confirming its reliability in accurately correlating electrical measurements with the stiffness degradation of the joint.

In summary, the possibility of developing analytical models that link damage extent to electrical measurements in components is essential, since it would not only enhance the effectiveness of health monitoring in composite parts but also aid in designing optimal material solutions for specific applications.

15480569, 0, Downloaded from https://4spepublications.onlinelibrary.wiley.com/doi/10.1002/pc.70332, Wiley Online Library on [26/08/2025]. See the Terms and Conditions (https://onlinelibrary.wiley.com/terms-and-conditions) on Wiley Online Library for rules of use; OA articles are governed by the applicable Creative Commons License

7 | Conclusions and Perspectives

The present review aims at supplying a summary of the most recent advancements for the surface modification of GF with carbon-based electrically conductive filler, with the ambition to provide some methodological hints for a more profitable design of GFRP systems for SHM solutions with enhanced sensing efficiency and remarkable mechanical features simultaneously.

The portrait drawn from the literature survey reveals that such attempts in the surface modification of GF and filler must address two key challenges: preventing the physical detachment of rGO and CNT networks from the fiber surface and ensuring an easy scale-up of GFRP production to maintain cost-effectiveness, sustainability, and performance.

In light of these observations, physical methods offer the significant advantage of scalability, but they entail the stringent and not so easy prerequisite of providing suitable conditions for carbon fillers dispersion and percolation in the epoxy matrices, essential requirements upon deposition for imparting the electrical conductivity to the GFRP component. Conversely, chemical grafting of CNTs and rGO directly on GF stands out as much more promising, thanks to the ability to finely control the hybrid interface through customizable surface functionalization. This approach, on the one hand, enhances adhesion properties by effectively preventing filler leaching; on the other hand, it promotes a uniform distribution and dispersion of carbon-based fillers, which is essential for the formation of a conductive network crucial to self-sensing functionality. Nevertheless, scaling up this strategy remains challenging due to several practical limitations.

Within the debate regarding the best method to employ, we may propose some compromise strategies, which combine the advantages of both physical and chemical methods. For example, the use of ceramic materials (e.g., silica, aluminum oxide) could serve as carriers for carbon-based fillers within the epoxy resin and promote interaction with the glass fiber surface. In fact, ceramic particles can be readily functionalized with CNTs and rGO units through well-established chemical grafting methods; subsequently, they can be incorporated into the epoxy resin, which can then be applied to glass fibers using physical techniques such as spray coating or dip coating.

Another valuable possibility is to exploit dual surface functionalization techniques: an initial modification of GF with ceramic nanoparticles to enrich their surface with suitable anchoring groups (e.g., —OH), followed by silanization of the modified fibers to facilitate the grafting of rGO and CNTs. Both these strategies are currently under investigation within our group.

As concerns the tests for the evaluation of the fiber/matrix interfacial adhesion of the composites, some critical observations must be made. Micro-scale techniques, such as the single fiber pull-out and microdroplet tests, exhibit high sensitivity and enable a direct assessment of the interfacial properties. However, experimental procedures can be difficult and may produce inconsistent results. In contrast, macro-scale methods like SBS test offer more scalable, standardized, and reproducible results but lack in terms of sensitivity at the micro-scale in describing the interface. Therefore, a comprehensive overview of material characteristics requires a complementary characterization approach at both micro and macro scales.

Finally, as evidenced in the text, while electrical health monitoring (EHM) in CFRP systems is more straightforward owing to the along-fiber high conductivity, which yields excellent sensitivity to fiber failure and delamination, for GFRPs, it is tightly connected to the modification of GF with conductive filler.

In general, proper electrode techniques (four-probe methods are usually used to minimize contact resistances) and meticulous surface preparation (such as superficial resin removal in CFRPs) are essential for reliable measurements.

Author Contributions

Marta Colombo: investigation, writing – original draft, writing – review and editing. **Silvia Mostoni:** conceptualization, writing – original draft, writing – review and editing, validation, supervision. **Giulia Fredi:** writing – review and editing, investigation. **Carol Rodricks:** investigation, writing – review and editing. **Gerhard Kalinka:** investigation, writing – review and editing. **Massimiliano Riva:** funding acquisition, visualization. **Andrea Vassallo:** funding acquisition, visualization. **Barbara Di Credico:** visualization, validation. **Roberto Scotti:** validation, visualization. **Michele Zappalorto:** investigation, writing – review and editing. **Massimiliano D'Arienzo:** writing – review and editing, writing – original draft, conceptualization, supervision.

Acknowledgments

UNIMIB and CRPI Srl acknowledge funding for an Innovative Industrial Doctoral Program Under the National Recovery and Resilience Plan (PNRR), Mission 4, Component 2 "From Research to Industry," Investment 3.3—of Italian Ministry of University and Research, funded by the European Union—NextGenerationEU. Open access publishing facilitated by Universita degli Studi di Milano-Bicocca, as part of the Wiley - CRUI-CARE agreement.

Conflicts of Interest

The authors declare no conflicts of interest.

Data Availability Statement

Data sharing not applicable to this article as no datasets were generated or analysed during the current study.

References

1. J. Chen, Z. Yu, and H. Jin, "Nondestructive Testing and Evaluation Techniques of Defects in Fiber-Reinforced Polymer Composites: A Review," *Frontiers in Materials* 9 (2022): 986645, https://doi.org/10.3389/fmats.2022.986645.

2. B. Wang, S. Zhong, T. Lee, K. Fancey, and J. Mi, "Non-Destructive Testing and Evaluation of Composite Materials/Structures: A State-of-the-Art Review," *Advances in Mechanical Engineering* 12 (2020): 168781402091376, https://doi.org/10.1177/1687814020913761.

3. S. Hassani, M. Mousavi, and A. H. Gandomi, "Structural Health Monitoring in Composite Structures: A Comprehensive Review," *Sensors* 22, no. 1 (2022): 153, https://doi.org/10.3390/s22010153.

15480569, 0, Downloaded from https://4spepublications.onlinelibrary.wiley.com/doi/10.1002/pc.70332, Wiley Online Library on [26/08/2025]. See the Terms and Conditions (https://onlinelibrary.wiley.com/terms-and-conditions) on Wiley Online Library for rules of use; OA articles are governed by the applicable Creative Commons License

4. K. S. Alblalaihid, S. A. Aldoihi, and A. A. Alharbi, "Structural Health Monitoring of Fiber Reinforced Composites Using Integrated a Linear Capacitance Based Sensor," *Polymers (Basel)* 16, no. 11 (2024): 1560, https://doi.org/10.3390/polym16111560.

5. L. Paleari, M. Bragaglia, F. Fabbrocino, and F. Nanni, "Structural Monitoring of Glass Fiber/Epoxy Laminates by Means of Carbon Nanotubes and Carbon Black Self-Monitoring Plies," *Nanomaterials* 11, no. 6 (2021): 1543, https://doi.org/10.3390/nano11061543.

6. S. Sethi and B. C. Ray, "Environmental Effects on Fibre Reinforced Polymeric Composites: Evolving Reasons and Remarks on Interfacial Strength and Stability," *Advances in Colloid and Interface Science* 217 (2015): 43–67, https://doi.org/10.1016/j.cis.2014.12.005.

7. J. D. H. Hughes, "The Carbon Fibre/Epoxy Interface—A Review," *Composites Science and Technology* 41, no. 1 (1991): 13–45, https://doi.org/10.1016/0266-3538(91)90050-Y.

8. Y. Zhou, M. Fan, and L. Chen, "Interface and Bonding Mechanisms of Plant Fibre Composites: An Overview," *Composites, Part B: Engineering* 101 (2016): 31–45, https://doi.org/10.1016/j.compositesb.2016.06.055.

9. I. Goda, E. Padayodi, and R. N. Raoelison, "Enhancing Fiber/Matrix Interface Adhesion in Polymer Composites: Mechanical Characterization Methods and Progress in Interface Modification," *Journal of Composite Materials* 58, no. 29 (2024): 3077–3110, https://doi.org/10.1177/00219983241283958.

10. S. J. Pickering, "Recycling Technologies for Thermoset Composite Materials—Current Status," *Composites. Part A, Applied Science and Manufacturing* 37, no. 8 (2006): 1206–1215, https://doi.org/10.1016/j.compositesa.2005.05.030.

11. M. C. S. Ribeiro, A. Fiúza, A. Ferreira, et al., "Recycling Approach Towards Sustainability Advance of Composite Materials' Industry," *Recycling* 1, no. 1 (2016): 178–193, https://doi.org/10.3390/recycling1010178.

12. E. Fitzer, R. Kleinholz, H. Tiesler, et al., "Fibers, 5. Synthetic Inorganic," in *Ullmann's Encyclopedia of Industrial Chemistry* (Wiley-VCH Verlag GmbH & Co. KGaA, 2008), https://doi.org/10.1002/14356007.a11_001.pub2.

13. K. K. Chawla, "Glass Fibers," in *Reference Module in Materials Science and Materials Engineering* (Elsevier, 2016), https://doi.org/10.1016/B978-0-12-803581-8.02325-0.

14. S. H. Kamarudin, M. S. Mohd Basri, M. Rayung, et al., "A Review on Natural Fiber Reinforced Polymer Composites (NFRPC) for Sustainable Industrial Applications," *Polymers (Basel)* 14, no. 17 (2022): 3698, https://doi.org/10.3390/polym14173698.

15. T. P. Sathishkumar, J. A. Naveen, and S. Satheeshkumar, "Hybrid Fiber Reinforced Polymer Composites—A Review," *Journal of Reinforced Plastics and Composites* 33 (2014): 454–471, https://doi.org/10.1177/0731684413516393.

16. M. Y. Khalid, A. Al Rashid, Z. U. Arif, M. F. Sheikh, H. Arshad, and M. A. Nasir, "Tensile Strength Evaluation of Glass/Jute Fibers Reinforced Composites: An Experimental and Numerical Approach," *Results in Engineering* 10 (2021): 100232, https://doi.org/10.1016/j.rineng.2021.100232.

17. M. M. Thwe and K. Liao, "Durability of Bamboo-Glass Fiber Reinforced Polymer Matrix Hybrid Composites," *Composites Science and Technology* 63, no. 3 (2003): 375–387, https://doi.org/10.1016/S0266-3538(02)00225-7.

18. S. B. Hosseini, "A Review: Nanomaterials as a Filler in Natural Fiber Reinforced Composites," *Journal of Natural Fibers* 14 (2016): 1–325, https://doi.org/10.1080/15440478.2016.1212765.

19. R. Malkapuram, V. Kumar, and Y. Negi, "Recent Development in Natural Fiber Reinforced Polypropylene Composites," *Journal of Reinforced Plastics and Composites* 28 (2009): 1169–1189, https://doi.org/10.1177/0731684407087759.

20. S. Panthapulakkal, L. C. Raghunanan, M. M. Sain, B. Kc, and J. Tjong, "Natural Fiber and Hybrid Fiber Thermoplastic Composites: Advancements in Lightweighting Applications," in *Green Composites* (Woodhead Publishing, 2017), https://api.semanticscholar.org/CorpusID:136123854.

21. M. Saleem, K. Orra, and V. Arumugam, "Structural Health Monitoring of Natural Fiber-Based Hybrid Composites," *Polymer Composites* 44, no. 9 (2023): 5867–5878, https://doi.org/10.1002/pc.27533.

22. A. B. Nair and R. Joseph, "Eco-Friendly Bio-Composites Using Natural Rubber (NR) Matrices and Natural Fiber Reinforcements," in *Chemistry, Manufacture and Applications of Natural Rubber* (Woodhead Publishing, 2014), 249–283, https://doi.org/10.1533/9780857096913.2.249.

23. D. A. Bhagwan, J. Lawrence, and K. Broutman Chandrashekhara, *Analysis_and_Performance_of_Fiber_Compos* (John Wiley and Sons, 2017).

24. M. Miwa and N. Horiba, "Effects of Fibre Length on Tensile Strength of Carbon/Glass Fibre Hybrid Composites," *Journal of Materials Science* 29 (1994): 973–977.

25. D. D. L. Chung, "2—Introduction to Carbon Composites," in *Carbon Composites*, 2nd ed., ed. D. D. L. Chung (Butterworth-Heinemann, 2017), 88–160, https://doi.org/10.1016/B978-0-12-804459-9.00002-6.

26. D. K. Rajak, D. D. Pagar, P. L. Menezes, and E. Linul, "Fiber-Reinforced Polymer Composites: Manufacturing, Properties, and Applications," *Polymers (Basel)* 11, no. 10 (2019): 1667, https://doi.org/10.3390/polym11101667.

27. T. P. Sathishkumar, S. Satheeshkumar, and J. Naveen, "Glass Fiber-Reinforced Polymer Composites—A Review," *Journal of Reinforced Plastics and Composites* 33, no. 13 (2014): 1258–1275, https://doi.org/10.1177/0731684414530790.

28. R. H. Doremus, *Glass Science* (Wiley, 1973), http://books.google.com/books?id=Y8dTAAAAMAAJ.

29. L. D. Pye, H. J. Stevens, J. Harrie, and W. C. LaCourse, *Introduction to Glass Science Proceedings of a Tutorial Symposium Held at the State University of New York, College of Ceramics at Alfred University, Alfred, N.Y., June 8–19, 1970* (Plenum Press, 1972), https://searchworks.stanford.edu/view/10479113.

30. L. Holland, *The Properties of Glass Surfaces* (Chapman & Hall, 1966).

31. C. G. Pantano, L. A. Carman, and S. Warner, "Glass Fiber Surface Effects in Silane Coupling," *Journal of Adhesion Science and Technology* 6, no. 1 (1992): 49–60, https://doi.org/10.1163/156856192X00043.

32. J. G. Matisons, "Silanes and Siloxanes as Coupling Agents to Glass: A Perspective," in *Silicone Surface Science*, ed. M. J. Owen and P. R. Dvornic (Springer Netherlands, 2012), 281–298, https://doi.org/10.1007/978-94-007-3876-8_10.

33. J. Dong, M. Chen, and J. Wang, "Recycling and Optimum Utilization of GFRP Waste Into Low-Carbon Geopolymer Paste for Sustainable Development," *Journal of Building Engineering* 97 (2024): 110867, https://doi.org/10.1016/j.jobe.2024.110867.

34. Y. Tao, S. A. Hadigheh, and Y. Wei, "Recycling of Glass Fibre Reinforced Polymer (GFRP) Composite Wastes in Concrete: A Critical Review and Cost Benefit Analysis," *Structure* 53 (2023): 1540–1556, https://doi.org/10.1016/j.istruc.2023.05.018.

35. J. Qureshi, "A Review of Recycling Methods for Fibre Reinforced Polymer Composites," *Sustainability* 14, no. 24 (2022): 16855, https://doi.org/10.3390/su142416855.

36. S. Yıldız, B. Karaağaç, and S. G. Güzeliş, "Utilization of Glass Fiber Reinforced Polymer Wastes," *Polymer Composites* 42, no. 1 (2021): 412–423, https://doi.org/10.1002/pc.25834.

37. A. Avila and D. Morais, "A Multiscale Investigation Based on Variance Analysis for Hand Lay-Up Composite Manufacturing,"

15480569, 0, Downloaded from https://4spepublications.onlinelibrary.wiley.com/doi/10.1002/pc.70332, Wiley Online Library on [26/08/2025]. See the Terms and Conditions (https://onlinelibrary.wiley.com/terms-and-conditions) on Wiley Online Library for rules of use; OA articles are governed by the applicable Creative Commons License

Composites Science and Technology 65 (2005): 827–838, https://doi.org/10.1016/j.compscitech.2004.05.021.

38. S. J. Kim, K. Pandey, D. Poddar, and H. M. Yoo, "In Situ Fabrication of Poly-l-Lactide & Its Application as a Glass Fiber Polymer Composites Using Resin Transfer Molding," *Polymer Composites* 46, no. 4 (2025): 3251–3263, https://doi.org/10.1002/pc.29167.

39. M. R. Ricciardi, V. Antonucci, M. Durante, et al., "A New Cost-Saving Vacuum Infusion Process for Fiber-Reinforced Composites: Pulsed Infusion," *Journal of Composite Materials* 48, no. 11 (2013): 1365–1373, https://doi.org/10.1177/0021998313485998.

40. S. M. R. Kazmi, Q. Govignon, and S. Bickerton, "Control of Laminate Quality for Parts Manufactured Using the Resin Infusion Process," *Journal of Composite Materials* 53, no. 3 (2018): 327–343, https://doi.org/10.1177/0021998318783308.

41. P. Mertiny, F. Ellyin, and A. Hothan, "An Experimental Investigation on the Effect of Multi-Angle Filament Winding on the Strength of Tubular Composite Structures," *Composites Science and Technology* 64, no. 1 (2004): 1–9, https://doi.org/10.1016/S0266-3538(03)00198-2.

42. A. H. Miller, N. Dodds, J. M. Hale, and A. G. Gibson, "High Speed Pultrusion of Thermoplastic Matrix Composites," *Composites. Part A, Applied Science and Manufacturing* 29, no. 7 (1998): 773–782, https://doi.org/10.1016/S1359-835X(98)00006-2.

43. M. D. Wakeman, T. A. Cain, C. D. Rudd, R. Brooks, and A. C. Long, "Compression Moulding of Glass and Polypropylene Composites for Optimised Macro- and Micro- Mechanical Properties—1 Commingled Glass and Polypropylene," *Composites Science and Technology* 58, no. 12 (1998): 1879–1898, https://doi.org/10.1016/S0266-3538(98)00011-6.

44. L. Zhang, X. Wang, P. Jingyu, and Y. Zhou, "Review of Automated Fibre Placement and Its Prospects for Advanced Composites," *Journal of Materials Science* 55, no. 17 (2020): 7121–7155, https://doi.org/10.1007/s10853-019-04090-7.

45. E. Oromiehie, G. Prusty, P. Compston, and G. Rajan, "Automated Fibre Placement Based Composite Structures: Review on the Defects, Impacts and Inspections Techniques," *Composite Structures* 224 (2019): 110987, https://doi.org/10.1016/j.compstruct.2019.110987.

46. B. Denkena, P. Horst, S. Heimbs, C. Schmidt, L. Reichert, and T. Tiemann, "Automated Fiber Placement: The Impact of Manufacturing Constraints on Achieving Structural Property Targets for CFRP-Stiffeners," *Procedia CIRP* 118 (2023): 845–850, https://doi.org/10.1016/j.procir.2023.06.145.

47. Y. Okuhara and H. Matsubara, "Carbon-Matrix Composites With Continuous Glass Fiber and Carbon Black for Maximum Strain Sensing," *Carbon* 45, no. 6 (2007): 1152–1159, https://doi.org/10.1016/j.carbon.2007.02.026.

48. A. G. David, R. Vimal Samsingh, and F. S. Esther, "A Rational Design of a Carbon Black Percolation Network Glass Fibers for Modeling an In Situ Self-Reporting Composite," *Proceedings of the Institution of Mechanical Engineers, Part L: Journal of Materials: Design and Applications* 238, no. 4 (2023): 739–753, https://doi.org/10.1177/14644207231208257.

49. T. N. Tallman, S. Gungor, K. W. Wang, and C. E. Bakis, "Damage Detection via Electrical Impedance Tomography in Glass Fiber/Epoxy Laminates With Carbon Black Filler," *Structural Health Monitoring* 14, no. 1 (2014): 100–109, https://doi.org/10.1177/1475921714554142.

50. G. Kraus, "Reinforcement of Elastomers by Carbon Black," *Rubber Chemistry and Technology* 51, no. 2 (1978): 297–321, https://doi.org/10.5254/1.3545836.

51. N. Rattanasom, T. Saowapark, and C. Deeprasertkul, "Reinforcement of Natural Rubber With Silica/Carbon Black Hybrid Filler," *Polymer Testing* 26, no. 3 (2007): 369–377, https://doi.org/10.1016/j.polymertesting.2006.12.003.

52. Z. Slanina, "The Science and Technology of Carbon Nanotubes K. Tanaka, T. Yamabe, K. Fukui, Eds.: Elsevier Science, Amsterdam, 1999," *Fullerene Science and Technology* 8, no. 6 (2000): 639–640, https://doi.org/10.1080/10641220009351440.

53. G. Mittal, V. Dhand, K. Y. Rhee, S. J. Park, and W. R. Lee, "A Review on Carbon Nanotubes and Graphene as Fillers in Reinforced Polymer Nanocomposites," *Journal of Industrial and Engineering Chemistry* 21 (2015): 11–25, https://doi.org/10.1016/j.jiec.2014.03.022.

54. H. Dai, E. W. Wong, and C. M. Lieber, "Probing Electrical Transport in Nanomaterials: Conductivity of Individual Carbon Nanotubes," *Science* 272, no. 5261 (1979): 523–526, https://doi.org/10.1126/science.272.5261.523.

55. L. Bokobza, "Multiwall Carbon Nanotube Elastomeric Composites: A Review," *Polymer (Guildford)* 48, no. 17 (2007): 4907–4920, https://doi.org/10.1016/j.polymer.2007.06.046.

56. Z. Ali, S. Yaqoob, J. Yu, and A. D'Amore, "Critical Review on the Characterization, Preparation, and Enhanced Mechanical, Thermal, and Electrical Properties of Carbon Nanotubes and Their Hybrid Filler Polymer Composites for Various Applications," *Composites Part C: Open Access* 13 (2024): 100434, https://doi.org/10.1016/j.jcomc.2024.100434.

57. T. Sisto, L. Zakharov, B. White, and R. Jasti, "Towards Pi-Extended Cycloparaphenylenes as Seeds for CNT Growth: Investigating Strain Relieving Ring-Openings and Rearrangements," *Chemical Science* 7 (2016): 3681–3688, https://doi.org/10.1039/C5SC04218F.

58. L. Boumia, M. Zidour, A. Benzair, and A. Tounsi, "A Timoshenko Beam Model for Vibration Analysis of Chiral Single-Walled Carbon Nanotubes," *Physica E, Low-Dimensional Systems & Nanostructures* 59 (2014): 186–191, https://doi.org/10.1016/j.physe.2014.01.020.

59. A. Lekawa-Raus, J. Patmore, L. Kurzepa, J. Bulmer, and K. Koziol, "Electrical Properties of Carbon Nanotube Based Fibers and Their Future Use in Electrical Wiring," *Advanced Functional Materials* 24, no. 24 (2014): 3661–3682, https://doi.org/10.1002/adfm.201303716.

60. D. Bhushan Kumar and G. Popli, "Carbon Nanotubes and Its Applications: A Review," 2015, 3, www.ijraset.com.

61. D. S. Bethune, C. H. Kiang, M. S. de Vries, et al., "Cobalt-Catalysed Growth of Carbon Nanotubes With Single-Atomic-Layer Walls," *Nature* 363, no. 6430 (1993): 605–607, https://doi.org/10.1038/363605a0.

62. C. Journet, W. K. Maser, P. Bernier, et al., "Large-Scale Production of Single-Walled Carbon Nanotubes by the Electric-Arc Technique," *Nature* 388, no. 6644 (1997): 756–758, https://doi.org/10.1038/41972.

63. K. Anazawa, K. Shimotani, C. Manabe, H. Watanabe, and M. Shimizu, "High-Purity Carbon Nanotubes Synthesis Method by an Arc Discharging in Magnetic Field," *Applied Physics Letters* 81, no. 4 (2002): 739–741, https://doi.org/10.1063/1.1491302.

64. N. Arora and N. N. Sharma, "Arc Discharge Synthesis of Carbon Nanotubes: Comprehensive Review," *Diamond and Related Materials* 50 (2014): 135–150, https://doi.org/10.1016/j.diamond.2014.10.001.

65. A. Thess, R. Lee, P. Nikolaev, et al., "Crystalline Ropes of Metallic Carbon Nanotubes," *Science* 273, no. 5274 (1979): 483–487, https://doi.org/10.1126/science.273.5274.483.

66. E. Muñoz, W. K. Maser, A. M. Benito, et al., "Single-Walled Carbon Nanotubes Produced by Cw CO_2-Laser Ablation: Study of Parameters Important for Their Formation," *Applied Physics A* 70, no. 2 (2000): 145–151, https://doi.org/10.1007/s003390050026.

67. M. Meyyappan, L. Delzeit, A. Cassell, and D. Hash, "Carbon Nanotube Growth by PECVD: A Review," *Plasma Sources Science and Technology* 12 (2003): 205–216.

68. S. Maruyama, R. Kojima, Y. Miyauchi, S. Chiashi, and M. Kohno, "Low-Temperature Synthesis of High-Purity Single-Walled Carbon Nanotubes From Alcohol," *Chemical Physics Letters* 360, no. 3 (2002): 229–234, https://doi.org/10.1016/S0009-2614(02)00838-2.

15480569, 0, Downloaded from https://4spepublications.onlinelibrary.wiley.com/doi/10.1002/pc.70332, Wiley Online Library on [26/08/2025]. See the Terms and Conditions (https://onlinelibrary.wiley.com/terms-and-conditions) on Wiley Online Library for rules of use; OA articles are governed by the applicable Creative Commons License

69. M. Su, B. Zheng, and J. Liu, "A Scalable CVD Method for the Synthesis of Single-Walled Carbon Nanotubes With High Catalyst Productivity," *Chemical Physics Letters* 322, no. 5 (2000): 321–326, https://doi.org/10.1016/S0009-2614(00)00422-X.

70. N. Saifuddin, A. Z. Raziah, and A. R. Junizah, "Carbon Nanotubes: A Review on Structure and Their Interaction With Proteins," *Journal of Chemistry* 2013, no. 1 (2013): 676815, https://doi.org/10.1155/2013/676815.

71. R. S. Hirlekar, M. Yamagar, H. Garse, M. Vij, V. J. Kadam, and B. Vidyapeeth, "Carbon Nanotubes and Its Applications: A Review," 2009, https://api.semanticscholar.org/CorpusID:16527754.

72. A. B. Suriani, R. M. Nor, and M. Rusop, "Vertically Aligned Carbon Nanotubes Synthesized From Waste Cooking Palm Oil," *Journal of the Ceramic Society of Japan* 118, no. 1382 (2010): 963–968, https://doi.org/10.2109/jcersj2.118.963.

73. K. K. Panchagnula and P. Kuppan, "Improvement in the Mechanical Properties of Neat GFRPs With Multi-Walled CNTs," *Journal of Materials Research and Technology* 8, no. 1 (2019): 366–376, https://doi.org/10.1016/j.jmrt.2018.02.009.

74. G. Y. Kim, G. Lee, and W. R. Yu, "Carbon-Nanotube-Grafted Glass-Fiber-Reinforced Composites: Synthesis and Mechanical Properties," *Heliyon* 10, no. 9 (2024): e30262, https://doi.org/10.1016/j.heliyon.2024.e30262.

75. M. Bhandari, J. Wang, D. Jang, I. Nam, and B. Huang, "A Comparative Study on the Electrical and Piezoresistive Sensing Characteristics of GFRP and CFRP Composites With Hybridized Incorporation of Carbon Nanotubes, Graphenes, Carbon Nanofibers, and Graphite Nanoplatelets," *Sensors* 21, no. 21 (2021): 7291, https://doi.org/10.3390/s21217291.

76. C. Sbarufatti, B. Patel, X. Fernández, et al., "Self-Sensing of CNT-Doped GFRP Panels During Impact and Compression After Impact Tests," in *European Workshop on Structural Health Monitoring* (Springer International Publishing, 2021), 527–536, https://doi.org/10.1007/978-3-030-64,908-1_49.

77. C. Buggisch, D. Gibhardt, N. Felmet, Y. Tetzner, and B. Fiedler, "Strain Sensing in GFRP via Fully Integrated Carbon Nanotube Epoxy Film Sensors," *Composites Part C: Open Access* 6 (2021): 100191, https://doi.org/10.1016/j.jcomc.2021.100191.

78. H. Zhang, E. Bilotti, and T. Peijs, "The Use of Carbon Nanotubes for Damage Sensing and Structural Health Monitoring in Laminated Composites: A Review," *Nano* 1, no. 4 (2015): 167–184, https://doi.org/10.1080/20550324.2015.1113639.

79. D. R. Dreyer, S. Park, C. W. Bielawski, and R. S. Ruoff, "The Chemistry of Graphene Oxide," *Chemical Society Reviews* 39, no. 1 (2010): 228–240, https://doi.org/10.1039/B917103G.

80. A. Gutiérrez-Cruz, A. R. Ruiz-Hernández, J. F. Vega-Clemente, D. G. Luna-Gazcón, and J. Campos-Delgado, "A Review of Top-Down and Bottom-Up Synthesis Methods for the Production of Graphene, Graphene Oxide and Reduced Graphene Oxide," *Journal of Materials Science* 57, no. 31 (2022): 14543–14578, https://doi.org/10.1007/s10853-022-07514-z.

81. K. K. H. De Silva, H. H. Huang, and M. Yoshimura, "Progress of Reduction of Graphene Oxide by Ascorbic Acid," *Applied Surface Science* 447 (2018): 338–346, https://doi.org/10.1016/j.apsusc.2018.03.243.

82. S. Park, J. An, J. R. Potts, A. Velamakanni, S. Murali, and R. S. Ruoff, "Hydrazine-Reduction of Graphite- and Graphene Oxide," *Carbon* 49, no. 9 (2011): 3019–3023, https://doi.org/10.1016/j.carbon.2011.02.071.

83. L. Huang, P. Zhu, G. Li, D. Lu, R. Sun, and C. P. Wong, "Core–Shell SiO 2 @RGO Hybrids for Epoxy Composites With Low Percolation Threshold and Enhanced Thermo-Mechanical Properties," *Journal of Materials Chemistry A* 2 (2014): 18246–18255, https://doi.org/10.1039/C4TA03702B.

84. A. Zhou, J. Bai, W. Hong, and H. Bai, "Electrochemically Reduced Graphene Oxide: Preparation, Composites, and Applications," *Carbon* 191 (2022): 301–332, https://doi.org/10.1016/j.carbon.2022.01.056.

85. M. Fathy, A. Gomaa, F. A. Taher, M. M. El-Fass, and A. E. H. B. Kashyout, "Optimizing the Preparation Parameters of GO and rGO for Large-Scale Production," *Journal of Materials Science* 51, no. 12 (2016): 5664–5675, https://doi.org/10.1007/s10853-016-9869-8.

86. S. Yang, W. Yue, D. Huang, C. Chen, H. Lin, and X. Yang, "A Facile Green Strategy for Rapid Reduction of Graphene Oxide by Metallic Zinc," *RSC Advances* 2, no. 23 (2012): 8827–8832, https://doi.org/10.1039/C2RA20746J.

87. Z. Fan, K. Wang, T. Wei, J. Yan, L. Song, and B. Shao, "An Environmentally Friendly and Efficient Route for the Reduction of Graphene Oxide by Aluminum Powder," *Carbon* 48, no. 5 (2010): 1686–1689, https://doi.org/10.1016/j.carbon.2009.12.063.

88. Z. J. Fan, W. Kai, J. Yan, et al., "Facile Synthesis of Graphene Nanosheets via Fe Reduction of Exfoliated Graphite Oxide," *ACS Nano* 5, no. 1 (2011): 191–198, https://doi.org/10.1021/nn102339t.

89. X. Fan, W. Peng, Y. Li, et al., "Deoxygenation of Exfoliated Graphite Oxide Under Alkaline Conditions: A Green Route to Graphene Preparation," *Advanced Materials* 20, no. 23 (2008): 4490–4493, https://doi.org/10.1002/adma.200801306.

90. C. Zhu, S. Guo, Y. Fang, and S. Dong, "Reducing Sugar: New Functional Molecules for the Green Synthesis of Graphene Nanosheets," *ACS Nano* 4, no. 4 (2010): 2429–2437, https://doi.org/10.1021/nn1002387.

91. H. Peng, L. Meng, L. Niu, and Q. Lu, "Simultaneous Reduction and Surface Functionalization of Graphene Oxide by Natural Cellulose With the Assistance of the Ionic Liquid," *Journal of Physical Chemistry C* 116, no. 30 (2012): 16294–16299, https://doi.org/10.1021/jp3043889.

92. M. J. Fernández-Merino, L. Guardia, J. I. Paredes, et al., "Vitamin C Is an Ideal Substitute for Hydrazine in the Reduction of Graphene Oxide Suspensions," *Journal of Physical Chemistry C* 114, no. 14 (2010): 6426–6432, https://doi.org/10.1021/jp100603h.

93. S. Bose, T. Kuila, A. K. Mishra, N. H. Kim, and J. H. Lee, "Dual Role of Glycine as a Chemical Functionalizer and a Reducing Agent in the Preparation of Graphene: An Environmentally Friendly Method," *Journal of Materials Chemistry* 22, no. 19 (2012): 9696–9703, https://doi.org/10.1039/C2JM00011C.

94. A. Migliavacca, S. Latorrata, P. Gallo Stampino, and G. Dotelli, "Preparation and Characterization of Graphene Oxide Based Membranes as Possible Gas Diffusion Layers for PEM Fuel Cells With Enhanced Surface Homogeneity," *Materials Today: Proceedings* 4, no. 11, Part 2 (2017): 11594–11607, https://doi.org/10.1016/j.matpr.2017.09.071.

95. S. Shabberhussain and V. Ramachandran, "Effect of Graphene Nanoplatelets on Mechanical Performance of GFRP Composites," *Materials Science Forum* 1059 (2022): 73–80, https://doi.org/10.4028/p-dm021j.

96. K. Malik, F. Ahmad, N. A. Yunus, et al., "The Effects of Graphene Hybridization on Mechanical Properties of GFRP Composites," 2401 (2021): 20023, https://doi.org/10.1063/5.0072598.

97. T. Topkaya, Y. H. Çelik, and E. Kilickap, "Mechanical Properties of Fiber/Graphene Epoxy Hybrid Composites," *Journal of Mechanical Science and Technology* 34, no. 11 (2020): 4589–4595, https://doi.org/10.1007/s12206-020-1016-4.

98. V. G. S. Veerakumar, B. P. Shanmugavel, and S. Harish, "On the Influence of the Functionalization of Graphene Nanoplatelets and Glass Fiber on the Mechanical Properties of GFRP Composites," *Applied Composite Materials* 28, no. 4 (2021): 1127–1152, https://doi.org/10.1007/s10443-021-09908-9.

99. A. Mirabedini, A. Ang, M. Nikzad, B. Fox, K. T. Lau, and N. Hameed, "Evolving Strategies for Producing Multiscale Graphene-Enhanced

15480569, 0, Downloaded from https://4spepublications.onlinelibrary.wiley.com/doi/10.1002/pc.70332, Wiley Online Library on [26/08/2025]. See the Terms and Conditions (https://onlinelibrary.wiley.com/terms-and-conditions) on Wiley Online Library for rules of use; OA articles are governed by the applicable Creative Commons License

Fiber-Reinforced Polymer Composites for Smart Structural Applications," *Advanced Science* 7, no. 11 (2020): 1903501, https://doi.org/10.1002/advs.201903501.

100. Q. Wang, Y. Tian, A. Duongthipthewa, et al., "An Embedded Non-Intrusive Graphene/Epoxy Broadband Nanocomposite Sensor Co-Cured With GFRP for In Situ Structural Health Monitoring," *Composites Science and Technology* 236 (2023): 109995, https://doi.org/10.1016/j.compscitech.2023.109995.

101. M. Anas, M. A. Nasir, Z. Asfar, S. Nauman, M. Akalin, and F. Ahmad, "Structural Health Monitoring of GFRP Laminates Using Graphene-Based Smart Strain Gauges," *Journal of the Brazilian Society of Mechanical Sciences and Engineering* 40, no. 8 (2018): 397, https://doi.org/10.1007/s40430-018-1320-4.

102. S. K. Singh, B. Nayak, T. J. Singh, and S. Halder, "Investigating the Role of Synthesized Reduced Graphene Oxide and Graphite Micro-Fillers on Mechanical and Fretting Wear Performance of Glass Fiber Epoxy-Based Composite," *High Performance Polymers* 35, no. 9 (2023): 946–962, https://doi.org/10.1177/09540083231196087.

103. M. Rafiee, F. Nitzsche, J. Laliberte, S. Hind, F. Robitaille, and M. R. Labrosse, "Thermal Properties of Doubly Reinforced Fiberglass/Epoxy Composites With Graphene Nanoplatelets, Graphene Oxide and Reduced-Graphene Oxide," *Composites Part B: Engineering* 164 (2019): 1–9, https://doi.org/10.1016/j.compositesb.2018.11.051.

104. S. Kesarwani, R. K. Verma, S. C. Jayswal, and P. Khare, "Investigation of Physiochemical and Mechanical Properties of Reduced Graphene Oxide (rGO) Modified Carbon Fiber Polymer Composites," *Journal of the Textile Institute* 115, no. 2 (2024): 188–200, https://doi.org/10.1080/00405000.2023.2200348.

105. M. S. S. Bathusha, I. U. Din, R. Umer, and K. A. Khan, "In Situ Monitoring of Crack Growth and Fracture Behavior in Composite Laminates Using Embedded Sensors of rGO Coated Fabrics and GnP Paper," *Sensors and Actuators A: Physical* 365 (2024): 114850, https://doi.org/10.1016/j.sna.2023.114850.

106. M. S. Nisha, S. M. Venthan, G. Rangasamy, et al., "Fabrication and Testing of rGO-PVDF Nanosensing Sheets on Glass Fibre-Reinforced Polymer for Structural Health Monitoring in Aerospace Engineering," *Applied Nanoscience* 13, no. 9 (2023): 5935–5947, https://doi.org/10.1007/s13204-023-02866-7.

107. M. Górski and M. Safuta, "Functional Carbon-Based Materials for Structural Health Monitoring and Protection of Concrete Structures," *Structural Concrete* (2024), https://doi.org/10.1002/suco.202400841.

108. Y. F. Fu, Y. Q. Li, Y. F. Liu, P. Huang, N. Hu, and S. Y. Fu, "High-Performance Structural Flexible Strain Sensors Based on Graphene-Coated Glass Fabric/Silicone Composite," *ACS Applied Materials & Interfaces* 10, no. 41 (2018): 35503–35509, https://doi.org/10.1021/acsami.8b09424.

109. A. Al-Sabagh, E. Taha, U. Kandil, et al., "Monitoring Moisture Damage Propagation in GFRP Composites Using Carbon Nanoparticles," *Polymers* 9, no. 3 (2017): 94, https://doi.org/10.3390/polym9030094.

110. S. Araby, Q. Meng, L. Zhang, I. Zaman, P. Majewski, and J. Ma, "Elastomeric Composites Based on Carbon Nanomaterials," *Nanotechnology* 26, no. 11 (2015): 112001, https://doi.org/10.1088/0957-4484/26/11/112001.

111. A. Sharma and S. C. Joshi, "Enhancement in Fatigue Performance of FRP Composites With Various Fillers: A Review," *Composite Structures* 309 (2023): 116724, https://doi.org/10.1016/j.compstruct.2023.116724.

112. B. G. Cho, S. H. Hwang, M. Park, J. K. Park, Y. B. Park, and H. G. Chae, "The Effects of Plasma Surface Treatment on the Mechanical Properties of Polycarbonate/Carbon Nanotube/Carbon Fiber Composites," *Composites Part B: Engineering* 160 (2019): 436–445, https://doi.org/10.1016/j.compositesb.2018.12.062.

113. Y. Kusano, S. V. Singh, K. Norrman, et al., "Ultrasound Enhanced Plasma Surface Modification at Atmospheric Pressure," *Surface Engineering* 28, no. 6 (2012): 453–457, https://doi.org/10.1179/174329441lY.0000000084.

114. W. K. Ng, M. Johar, H. A. Israr, and K. J. Wong, "7—A Review on the Interfacial Characteristics of Natural Fibre Reinforced Polymer Composites," in *Interfaces in Particle and Fibre Reinforced Composites*, ed. K. L. Goh, M. K. A, R. T. De Silva, and S. Thomas (Woodhead Publishing, 2020), 163–198, https://doi.org/10.1016/B978-0-08-102665-6.00007-8.

115. A. Rajeswari, E. Jackcina Stobel Christy, S. Gopi, K. Jayaraj, and A. Pius, "9—Characterization Studies of Polymer-Based Composites Related to Functionalized Filler-Matrix Interface," in *Interfaces in Particle and Fibre Reinforced Composites*, ed. K.-L. Goh, S. Thomas, R. T. De Silva, and M. K. Aswathi (Woodhead Publishing, 2020), 219–250, https://doi.org/10.1016/B978-0-08-102665-6.00009-1.

116. W. Li, A. Dichiara, and J. Bai, "Carbon Nanotube–Graphene Nanoplatelet Hybrids as High-Performance Multifunctional Reinforcements in Epoxy Composites," *Composites Science and Technology* 74 (2013): 221–227, https://doi.org/10.1016/j.compscitech.2012.11.015.

117. R. P. Behera, P. Rawat, K. K. Singh, C. Kumar, and A. Deep, "Flexural and Short Beam Shear Strength Analysis of Symmetrical GFRP Composites Reinforced With MWCNTs Having Notches," *IOP Conference Series: Materials Science and Engineering* 377 (2018): 012147, https://doi.org/10.1088/1757-899X/377/1/012147.

118. X. L. Xie, Y. W. Mai, and X. P. Zhou, "Dispersion and Alignment of Carbon Nanotubes in Polymer Matrix: A Review," *Materials Science & Engineering R: Reports* 49, no. 4 (2005): 89–112, https://doi.org/10.1016/j.mser.2005.04.002.

119. H. Kim, Y. Miura, and C. W. Macosko, "Graphene/Polyurethane Nanocomposites for Improved Gas Barrier and Electrical Conductivity," *Chemistry of Materials* 22, no. 11 (2010): 3441–3450, https://doi.org/10.1021/cm100477v.

120. J. F. Feller and Y. Grohens, "Coupling Ability of Silane Grafted Poly(Propene) at Glass Fibers/Poly(Propene) Interface," *Composites. Part A, Applied Science and Manufacturing* 35, no. 1 (2004): 1–10, https://doi.org/10.1016/j.compositesa.2003.10.001.

121. J. Thomason, "A Review of the Analysis and Characterisation of Polymeric Glass Fibre Sizings," *Polymer Testing* 85 (2020): 106421, https://doi.org/10.1016/j.polymertesting.2020.106421.

122. R. L. Gorowara, W. E. Kosik, S. H. McKnight, and R. L. McCullough, "Molecular Characterization of Glass Fiber Surface Coatings for Thermosetting Polymer Matrix/Glass Fiber Composites," *Composites Part A, Applied Science and Manufacturing* 32, no. 3 (2001): 323–329, https://doi.org/10.1016/S1359-835X(00)00112-3.

123. J. L. Thomason, U. Nagel, L. Yang, and D. Bryce, "A Study of the Thermal Degradation of Glass Fibre Sizings at Composite Processing Temperatures," *Composites. Part A, Applied Science and Manufacturing* 121 (2019): 56–63, https://doi.org/10.1016/j.compositesa.2019.03.013.

124. S. Singh, Z. Kamble, and G. Neje, "Electro-Mechanical Behavior of Self-Sensing Textile-Reinforced Composites for In Situ Structural Health Monitoring," *Journal of Reinforced Plastics and Composites* 43 (2023): 1205–1213, https://doi.org/10.1177/07316844231202370.

125. G. Uribe-Riestra, P. Ayuso-Faber, M. Rivero-Ayala, J. Cauich-Cupul, F. Gamboa, and F. Avilés, "Structural Health Monitoring of Carbon Nanotube-Modified Glass Fiber-Reinforced Polymer Composites by Electrical Resistance Measurements and Digital Image Correlation," *Structural Health Monitoring* 23, no. 1 (2024): 555–567, https://doi.org/10.1177/14759217231173439.

126. S. L. Gao, R. C. Zhuang, J. Zhang, J. W. Liu, and E. Mäder, "Class Fibers With Carbon Nanotube Networks as Multifunctional Sensors,"

15480569, 0, Downloaded from https://4spepublications.onlinelibrary.wiley.com/doi/10.1002/pc.70332, Wiley Online Library on [26/08/2025]. See the Terms and Conditions (https://onlinelibrary.wiley.com/terms-and-conditions) on Wiley Online Library for rules of use; OA articles are governed by the applicable Creative Commons License

Advanced Functional Materials 20, no. 12 (2010): 1885–1893, https://doi.org/10.1002/adfm.201000283.

127. K. Wen, Y. Liu, S. Huang, X. Su, C. Liang, and G. Zhao, "Achieving Broadband Microwave Absorption and Excellent Mechanical Properties via Constructing 3D Reduced Graphene Oxide Networks in Glass Fiber/Epoxy Resin Composites," *Composites Science and Technology* 229 (2022): 109666, https://doi.org/10.1016/j.compscitech.2022.109666.

128. R. Moriche, A. Jiménez-Suárez, M. Sánchez, S. G. Prolongo, and A. Ureña, "Graphene Nanoplatelets Coated Glass Fibre Fabrics as Strain Sensors," *Composites Science and Technology* 146 (2017): 59–64, https://doi.org/10.1016/j.compscitech.2017.04.019.

129. S. Bhattacharjee, C. R. Macintyre, P. Bahl, et al., "Reduced Graphene Oxide and Nanoparticles Incorporated Durable Electroconductive Silk Fabrics," *Advanced Materials Interfaces* 7, no. 20 (2020): 2000814, https://doi.org/10.1002/admi.202000814.

130. R. Balaji and M. Sasikumar, "Graphene Based Strain and Damage Prediction System for Polymer Composites," *Composites. Part A, Applied Science and Manufacturing* 103 (2017): 48–59, https://doi.org/10.1016/j.compositesa.2017.09.006.

131. C. Cao, Z. Lin, X. Liu, et al., "Strong Reduced Graphene Oxide Coated *Bombyx mori* Silk," *Advanced Functional Materials* 31, no. 34 (2021): 2102923, https://doi.org/10.1002/adfm.202102923.

132. R. Cherrington and J. Liang, "2—Materials and Deposition Processes for Multifunctionality," in *Design and Manufacture of Plastic Components for Multifunctionality*, ed. V. Goodship, B. Middleton, and R. Cherrington (William Andrew Publishing, 2016), 19–51, https://doi.org/10.1016/B978-0-323-34061-8.00002-8.

133. X. Ren, H. Zou, Q. Diao, et al., "Surface Modification Technologies for Enhancing the Tribological Properties of Cemented Carbides: A Review," *Tribology International* 180 (2023): 108257, https://doi.org/10.1016/j.triboint.2023.108257.

134. H. Qian, A. Bismarck, E. S. Greenhalgh, G. Kalinka, and M. S. P. Shaffer, "Hierarchical Composites Reinforced With Carbon Nanotube Grafted Fibers: The Potential Assessed at the Single Fiber Level," *Chemistry of Materials* 20, no. 5 (2008): 1862–1869, https://doi.org/10.1021/cm702782j.

135. M. F. De Riccardis, D. Carbone, T. D. Makris, R. Giorgi, N. Lisi, and E. Salernitano, "Anchorage of Carbon Nanotubes Grown on Carbon Fibres," *Carbon* 44, no. 4 (2006): 671–674, https://doi.org/10.1016/j.carbon.2005.09.024.

136. H. Mahmood, L. Vanzetti, M. Bersani, and A. Pegoretti, "Mechanical Properties and Strain Monitoring of Glass-Epoxy Composites With Graphene-Coated Fibers," *Composites. Part A, Applied Science and Manufacturing* 107 (2018): 112–123, https://doi.org/10.1016/j.compositesa.2017.12.023.

137. J. Zhang, R. Zhuang, J. Liu, E. Mäder, G. Heinrich, and S. Gao, "Functional Interphases With Multi-Walled Carbon Nanotubes in Glass Fibre/Epoxy Composites," *Carbon* 48, no. 8 (2010): 2273–2281, https://doi.org/10.1016/j.carbon.2010.03.001.

138. H. Mahmood, A. Dorigato, and A. Pegoretti, "Temperature Dependent Strain/Damage Monitoring of Glass/Epoxy Composites With Graphene as a Piezoresistive Interphase," *Fibers* 7, no. 2 (2019): 17, https://doi.org/10.3390/fib7020017.

139. M. Li, P. Xiong, F. Yan, et al., "An Overview of Graphene-Based Hydroxyapatite Composites for Orthopedic Applications," *Bioactive Materials* 3, no. 1 (2018): 1–18, https://doi.org/10.1016/j.bioactmat.2018.01.001.

140. A. Chavez-Valdez, M. S. P. Shaffer, and A. R. Boccaccini, "Applications of Graphene Electrophoretic Deposition. A Review," *Journal of Physical Chemistry. B* 117, no. 6 (2013): 1502–1515, https://doi.org/10.1021/jp3064917.

141. J. Chen, J. Wu, H. Ge, D. Zhao, C. Liu, and X. Hong, "Reduced Graphene Oxide Deposited Carbon Fiber Reinforced Polymer Composites for Electromagnetic Interference Shielding," *Composites. Part A, Applied Science and Manufacturing* 82 (2016): 141–150, https://doi.org/10.1016/j.compositesa.2015.12.008.

142. H. Zhang, Y. Liu, M. Kuwata, E. Bilotti, and T. Peijs, "Improved Fracture Toughness and Integrated Damage Sensing Capability by Spray Coated CNTs on Carbon Fibre Prepreg," *Composites. Part A, Applied Science and Manufacturing* 70 (2015): 102–110, https://doi.org/10.1016/j.compositesa.2014.11.029.

143. M. Peñas-Caballero, E. Chemello, A. M. Grande, M. Hernández Santana, R. Verdejo, and M. A. Lopez-Manchado, "Poly(Ethylene-Co-Methacrylic Acid) Coated Carbon Fiber for Self-Healing Composites," *Composites. Part A, Applied Science and Manufacturing* 169 (2023): 107537, https://doi.org/10.1016/j.compositesa.2023.107537.

144. J. M. Vázquez-Moreno, R. Sánchez-Hidalgo, E. Sanz-Horcajo, J. Viña, R. Verdejo, and M. A. López-Manchado, "Preparation and Mechanical Properties of Graphene/Carbon Fiber-Reinforced Hierarchical Polymer Composites," *Journal of Composites Science* 3, no. 1 (2019): 30, https://doi.org/10.3390/jcs3010030.

145. A. Ojstršek, L. Jug, and O. Plohl, "A Review of Electro Conductive Textiles Utilizing the Dip-Coating Technique: Their Functionality, Durability and Sustainability," *Polymers (Basel)* 14, no. 21 (2022): 4713, https://doi.org/10.3390/polym14214713.

146. D. He, B. Fan, H. Zhao, et al., "Design of Electrically Conductive Structural Composites by Modulating Aligned CVD-Grown Carbon Nanotube Length on Glass Fibers," *ACS Applied Materials & Interfaces* 9, no. 3 (2017): 2948–2958, https://doi.org/10.1021/acsami.6b13397.

147. S. A. Steiner, III, R. Li, and B. L. Wardle, "Circumventing the Mechanochemical Origins of Strength Loss in the Synthesis of Hierarchical Carbon Fibers," *ACS Applied Materials & Interfaces* 5, no. 11 (2013): 4892–4903, https://doi.org/10.1021/am4006385.

148. S. Rahmanian, A. R. Suraya, R. Zahari, and E. S. Zainudin, "Synthesis of Vertically Aligned Carbon Nanotubes on Carbon Fiber," *Applied Surface Science* 271 (2013): 424–428, https://doi.org/10.1016/j.apsusc.2013.01.207.

149. Y. Xia, L. Zeng, W. Wang, et al., "Synthesis and Characterization of Carbon Nanotubes on Carbon Microfibers by Floating Catalyst Method," *Applied Surface Science* 253, no. 16 (2007): 6807–6810, https://doi.org/10.1016/j.apsusc.2007.01.129.

150. H. Z. Hui, D. S. Ming, H. J. Bao, et al., "Synthesis of Carbon Nanotubes on Carbon Fibers by Modified Chemical Vapor Deposition," *New Carbon Materials* 27, no. 5 (2012): 352–361, https://doi.org/10.1016/S1872-5805(12)60021-3.

151. M. Atiq Ur Rehman, Q. Chen, A. Braem, M. S. P. Shaffer, and A. R. Boccaccini, "Electrophoretic Deposition of Carbon Nanotubes: Recent Progress and Remaining Challenges," *International Materials Reviews* 66, no. 8 (2021): 533–562, https://doi.org/10.1080/09506608.2020.1831299.

152. M. Rafiee, F. Nitzsche, J. Laliberte, J. Thibault, and M. R. Labrosse, "Simultaneous Reinforcement of Matrix and Fibers for Enhancement of Mechanical Properties of Graphene-Modified Laminated Composites," *Polymer Composites* 40, no. S2 (2019): E1732–E1745, https://doi.org/10.1002/pc.25137.

153. A. T. Dibenedetto, "Tailoring of Interfaces in Glass Fiber Reinforced Polymer Composites: A Review," *Materials Science and Engineering A* 302 (2001): 74–82.

154. U. Schubert and N. Hüsing, *Synthesis of Inorganic Materials* (Wiley, 2012), https://books.google.it/books?id=hqA9Z8PEmu8C.

155. D. E. Leyden, *Silanes, Surfaces, and Interfaces: Proceedings of the Silanes, Surfaces, and Interfaces Symposium Snowmass, Colorado, June 19–21, 1985* (Gordon and Breach, 1986), https://books.google.it/books?id=lQDwAAAAMAAJ.

15480569, 0, Downloaded from https://4spepublications.onlinelibrary.wiley.com/doi/10.1002/pc.70332, Wiley Online Library on [26/08/2025]. See the Terms and Conditions (https://onlinelibrary.wiley.com/terms-and-conditions) on Wiley Online Library for rules of use; OA articles are governed by the applicable Creative Commons License

156. E. R. Pohl and F. D. Osterholtz, "Kinetics and Mechanism of Aqueous Hydrolysis and Condensation of Alkyltrialkoxysilanes," in *Molecular Characterization of Composite Interfaces*, ed. H. Ishida and G. Kumar (Springer US, 1985), 157–170, https://doi.org/10.1007/978-1-4899-2251-9_10.

157. A. A. Issa and A. S. Luyt, "Kinetics of Alkoxysilanes and Organoalkoxysilanes Polymerization: A Review," *Polymers (Basel)* 11, no. 3 (2019): 537, https://doi.org/10.3390/polym11030537.

158. E. P. Plueddemann, *Silanes and Other Coupling Agents*, ed. Klm (Springer, 1992), https://doi.org/10.1007/978-1-4899-2070-6.

159. C. C. Le-Huy, L. G. Britcher, and J. G. Matisons, "The Effect of Silane Concentration on the Adsorption of Poly(Vinyl Acetate-Co-Maleate) and γ-Methacryloxypropyl- Trimethoxysilane Onto E-Glass Fibers," *Silicon Chemistry* 1, no. 3 (2002): 195–205, https://doi.org/10.1023/A:1021298328215.

160. H. Lee, D. E. Yoon, S. Koh, M. S. Kang, J. Lim, and D. C. Lee, "Ligands as a Universal Molecular Toolkit in Synthesis and Assembly of Semiconductor Nanocrystals," *Chemical Science* 11, no. 9 (2020): 2318–2329, https://doi.org/10.1039/C9SC05200C.

161. K. Bhattacharjee and B. L. V. Prasad, "Surface Functionalization of Inorganic Nanoparticles With Ligands: A Necessary Step for Their Utility," *Chemical Society Reviews* 52, no. 8 (2023): 2573–2595, https://doi.org/10.1039/D1CS00876E.

162. V. M. Karbhari, M. Engineer, and I. I. D. A. Eckel, "On the Durability of Composite Rehabilitation Schemes for Concrete: Use of a Peel Test," 32, no. 1 (1997): 147–156, https://doi.org/10.1023/A:1018591619404.

163. V. M. Miettinen, K. K. Narva, and P. K. Vallittu, "Water Sorption, Solubility and Effect of Post-Curing of Glass Fibre Reinforced Polymers," *Biomaterials* 20, no. 13 (1999): 1187–1194, https://doi.org/10.1016/S0142-9612(99)00003-4.

164. M. Woo and M. R. Piggott, "Water Absorption of Resins and Composites: Iv. Water Transport in Fiber Reinforced Plastics," *Journal of Composites Technology & Research* 10, no. 1 (1988): 20–24, https://doi.org/10.1520/ctr10271j.

165. F. Ellyin and C. Rohrbacher, "The Influence of Aqueous Environment, Temperature and Cyclic Loading on Glass-Fibre/Epoxy Composite Laminates," *Journal of Reinforced Plastics and Composites* 22, no. 7 (2003): 615–636, https://doi.org/10.1177/0731684403027609.

166. S. Birger, A. Moshonov, and S. Kenig, "The Effects of Thermal and Hygrothermal Ageing on the Failure Mechanisms of Graphite-Fabric Epoxy Composites Subjected to Flexural Loading," *Composites* 20, no. 4 (1989): 341–348, https://doi.org/10.1016/0010-4361(89)90659-9.

167. B. C. Ray, "Effects of Changing Environment and Loading Speed on Mechanical Behavior of FRP Composites," *Journal of Reinforced Plastics and Composites* 25, no. 12 (2006): 1227–1240, https://doi.org/10.1177/0731684406059783.

168. B. C. Ray and D. Rathore, "Durability and Integrity Studies of Environmentally Conditioned Interfaces in Fibrous Polymeric Composites: Critical Concepts and Comments," *Advances in Colloid and Interface Science* 209 (2014): 68–83, https://doi.org/10.1016/j.cis.2013.12.014.

169. X. He, F. Zhang, R. Wang, and W. Liu, "Preparation of a Carbon Nanotube/Carbon Fiber Multi-Scale Reinforcement by Grafting Multi-Walled Carbon Nanotubes Onto the Fibers," *Carbon* 45, no. 13 (2007): 2559–2563, https://doi.org/10.1016/j.carbon.2007.08.018.

170. A. Laachachi, A. Vivet, G. Nouet, et al., "A Chemical Method to Graft Carbon Nanotubes Onto a Carbon Fiber," *Materials Letters* 62, no. 3 (2008): 394–397, https://doi.org/10.1016/j.matlet.2007.05.044.

171. A. Vivet, D. B. Ben, C. Poilâne, J. Chen, and M. Ayachi, "A Method for the Chemical Anchoring of Carbon Nanotubes Onto Carbon Fibre and Its Impact on the Strength of Carbon Fibre Composites," *Journal of Materials Science* 46, no. 5 (2011): 1322–1327, https://doi.org/10.1007/s10853-010-4919-0.

172. Q. Peng, X. He, Y. Li, et al., "Chemically and Uniformly Grafting Carbon Nanotubes Onto Carbon Fibers by Poly(Amidoamine) for Enhancing Interfacial Strength in Carbon Fiber Composites," *Journal of Materials Chemistry* 22, no. 13 (2012): 5928–5931, https://doi.org/10.1039/C2JM16723A.

173. F. Zhao, Y. Huang, L. Liu, Y. Bai, and L. Xu, "Formation of a Carbon Fiber/Polyhedral Oligomeric Silsesquioxane/Carbon Nanotube Hybrid Reinforcement and Its Effect on the Interfacial Properties of Carbon Fiber/Epoxy Composites," *Carbon* 49, no. 8 (2011): 2624–2632, https://doi.org/10.1016/j.carbon.2011.02.026.

174. L. Tzounis, M. Kirsten, F. Simon, E. Mäder, and M. Stamm, "The Interphase Microstructure and Electrical Properties of Glass Fibers Covalently and Non-Covalently Bonded With Multiwall Carbon Nanotubes," *Carbon* 73 (2014): 310–324, https://doi.org/10.1016/j.carbon.2014.02.069.

175. V. Eskizeybek, A. Avcı, and A. Gülce, "Preparation and Mechanical Properties of Carbon Nanotube Grafted Glass Fabric/Epoxy Multi-Scale Composites," *Advanced Composite Materials* 26, no. 2 (2017): 169–180, https://doi.org/10.1080/09243046.2015.1052188.

176. J. Fang, L. Zhang, and C. Li, "Largely Enhanced Transcrystalline Formation and Properties of Polypropylene on the Surface of Glass Fiber as Induced by PEI-CNT and PEI-GO Modification," *Polymer (Guildf)* 186 (2020): 122025, https://doi.org/10.1016/j.polymer.2019.122025.

177. J. Fang, L. Zhang, and C. Li, "Polyamide 6 Composite With Highly Improved Mechanical Properties by PEI-CNT Grafted Glass Fibers Through Interface Wetting, Infiltration and Crystallization," *Polymer (Guildford)* 172 (2019): 253–264, https://doi.org/10.1016/j.polymer.2019.03.013.

178. J. Chen, D. Zhao, X. Jin, C. Wang, D. Wang, and H. Ge, "Modifying Glass Fibers With Graphene Oxide: Towards High-Performance Polymer Composites," *Composites Science and Technology* 97 (2014): 41–45, https://doi.org/10.1016/j.compscitech.2014.03.023.

179. Y. Hua, F. Li, Y. Liu, et al., "Positive Synergistic Effect of Graphene Oxide/Carbon Nanotube Hybrid Coating on Glass Fiber/Epoxy Interfacial Normal Bond Strength," *Composites Science and Technology* 149 (2017): 294–304, https://doi.org/10.1016/j.compscitech.2017.06.024.

180. S. AhmadvashAghbash, I. Verpoest, Y. Swolfs, and M. Mehdikhani, "Methods and Models for Fibre–Matrix Interface Characterisation in Fibre-Reinforced Polymers: A Review," *International Materials Reviews* 68, no. 8 (2023): 1245–1319, https://doi.org/10.1080/09506608.2023.2265701.

181. P. J. Herrera-Franco and L. T. Drzal, "Comparison of Methods for the Measurement of Fibre/Matrix Adhesion in Composites," *Composites* 23, no. 1 (1992): 2–27, https://doi.org/10.1016/0010-4361(92)90282-Y.

182. S. Huang, Q. Fu, L. Yan, and B. Kasal, "Characterization of Interfacial Properties Between Fibre and Polymer Matrix in Composite Materials—A Critical Review," *Journal of Materials Research and Technology* 13 (2021): 1441–1484, https://doi.org/10.1016/j.jmrt.2021.05.076.

183. G. Fredi, A. Dorigato, S. Unterberger, N. Artuso, and A. Pegoretti, "Discontinuous Carbon Fiber/Polyamide Composites With Microencapsulated Paraffin for Thermal Energy Storage," *Journal of Applied Polymer Science* 136, no. 16 (2019): 47408, https://doi.org/10.1002/app.47408.

184. M. Valentini, O. De Almeida, M. Kakkonen, et al., "Effect of Fiber Surface State on the Thermomechanical and Interfacial Properties of In Situ Polymerized Polyamide 6/Basalt Fiber Composites," *Composites. Part A, Applied Science and Manufacturing* 190 (2025): 108681, https://doi.org/10.1016/j.compositesa.2024.108681.

15480569, 0, Downloaded from https://4spepublications.onlinelibrary.wiley.com/doi/10.1002/pc.70332, Wiley Online Library on [26/08/2025]. See the Terms and Conditions (https://onlinelibrary.wiley.com/terms-and-conditions) on Wiley Online Library for rules of use; OA articles are governed by the applicable Creative Commons License

185. C. W. Rodricks, I. Greenfeld, B. Fiedler, and H. D. Wagner, "Fragmentation of Beaded Fibres in a Composite," *Materials* 15, no. 3 (2022): 890, https://doi.org/10.3390/ma15030890.

186. S. Deng, L. Ye, Y. W. Mai, and H. Y. Liu, "Evaluation of Fibre Tensile Strength and Fibre/Matrix Adhesion Using Single Fibre Fragmentation Tests," *Composites. Part A, Applied Science and Manufacturing* 29, no. 4 (1998): 423–434, https://doi.org/10.1016/S1359-835X(97)00094-8.

187. Y. I. Yilmaz, "Analyzing Single Fiber Fragmentation Test Data by Using Stress Transfer Model," *Journal of Composite Materials* 36, no. 5 (2002): 537–551, https://doi.org/10.1177/0021998302036005465.

188. M. Zhu, Y. Wang, C. Wang, F. Chen, and Q. Liu, "An Improved Analytical Model for Inversely Determining Multiple Interfacial Parameters From Single Fiber Micro-Raman and Fragmentation Tests," *Composites Science and Technology* 214 (2021): 108983, https://doi.org/10.1016/j.compscitech.2021.108983.

189. T. Xiao, Y. Wang, and H. Xiong, "Development of a New Device for Single Fiber Fragmentation Tests," in *2015 8th International Congress on Image and Signal Processing (CISP)* (IEEE, 2015), 909–913, https://doi.org/10.1109/CISP.2015.7408007.

190. G. Pandey, C. H. Kareliya, and R. P. Singh, "A Study of the Effect of Experimental Test Parameters on Data Scatter in Microbond Testing," *Journal of Composite Materials* 46, no. 3 (2011): 275–284, https://doi.org/10.1177/0021998311410508.

191. A. Martone, S. Iacono S Dello, A. Zamani, et al., "Modelling of the Micro-Bond Test for Mechanical Analysis of the Fibre/Matrix Interphase in Fibre Reinforced Plastics," in *AIP Conference Proceedings*, vol. 2196 (AIP Publishing LLC, 2019), 20041, https://doi.org/10.1063/1.5140314.

192. S. Sockalingam and G. Nilakantan, "Fiber-Matrix Interface Characterization Through the Microbond Test," *International Journal of Aeronautical and Space Sciences* 13 (2012): 282–295, https://doi.org/10.5139/IJASS.2012.13.3.282.

193. Q. Li, G. Nian, W. Tao, and S. Qu, "Size Effect on Microbond Testing Interfacial Shear Strength of Fiber-Reinforced Composites," *Journal of Applied Mechanics* 86, no. 7 (2019): 071004, https://doi.org/10.1115/1.4043354.

194. J. C. Zarges, C. Kaufhold, M. Feldmann, and H. P. Heim, "Single Fiber Pull-Out Test of Regenerated Cellulose Fibers in Polypropylene: An Energetic Evaluation," *Composites. Part A, Applied Science and Manufacturing* 105 (2018): 19–27, https://doi.org/10.1016/j.compositesa.2017.10.030.

195. A. Hampe, G. Kalinka, S. Meretz, and E. Schulz, "An Advanced Equipment for Single-Fibre Pull-Out Test Designed to Monitor the Fracture Process," *Composites* 26, no. 1 (1995): 40–46, https://doi.org/10.1016/0010-4361(94)P3628-E.

196. S. Doshi, A. Schneider, J. Deitzel, and J. Gillespie, Jr., "Interfacial Characterization of S2 Glass-Epoxy Resin Using Single Fiber Pullout Tests at Varying Temperature and Moisture Level," in *Proceedings of the 38th American Society for Composites Technical Conference* (DEStech Publications, 2023), 295–306, https://doi.org/10.12783/asc38/36643.

197. N. Christ, P. Gumbsch, and J. Hohe, "Single Fiber Pull-Out Investigation at Different Temperature and Humidity Conditions: Experimental Characterization of the Fiber-Matrix Interface in Carbon Fiber Reinforced Polyamide 6," *Journal of Thermoplastic Composite Materials* (2025): 08927057251314436, https://doi.org/10.1177/08927057251314436.

198. G. Kalinka, A. Leistner, and A. Hampe, "Characterisation of the Fibre/Matrix Interface in Reinforced Polymers by the Push-In Technique," *Composites Science and Technology* 57, no. 8 (1997): 845–851, https://doi.org/10.1016/S0266-3538(96)00159-5.

199. J. Jäger, M. G. R. Sause, F. Burkert, J. Moosburger-Will, M. Greisel, and S. Horn, "Influence of Plastic Deformation on Single-Fiber Push-Out Tests of Carbon Fiber Reinforced Epoxy Resin," *Composites. Part A, Applied Science and Manufacturing* 71 (2015): 157–167, https://doi.org/10.1016/j.compositesa.2015.01.011.

200. B. Rohrmüller, P. Gumbsch, and J. Hohe, "Calibrating a Fiber–Matrix Interface Failure Model to Single Fiber Push-Out Tests and Numerical Simulations," *Composites. Part A, Applied Science and Manufacturing* 150 (2021): 106607, https://doi.org/10.1016/j.compositesa.2021.106607.

201. N. Chandra and H. Ghonem, "Interfacial Mechanics of Push-Out Tests: Theory and Experiments," *Composites Part A, Applied Science and Manufacturing* 32, no. 3 (2001): 575–584, https://doi.org/10.1016/S1359-835X(00)00051-8.

202. Z. Lei, G. Luo, W. Sun, et al., "Exploring the Iosipescu Method to Investigate Interlaminar Shear Fatigue Behavior and Failure Mechanisms of Carbon Fiber Reinforced Composites," *International Journal of Fatigue* 178 (2023): 108020, https://doi.org/10.1016/j.ijfatigue.2023.108020.

203. L. A. Carlsson, D. F. A, and R. B. Pipes, "Basic Experimental Characterization of Polymer Matrix Composite Materials," *Polymer Reviews* 53, no. 2 (2013): 277–302, https://doi.org/10.1080/15583724.2013.776588.

204. F. H. Gojny, M. H. G. Wichmann, B. Fiedler, W. Bauhofer, and K. Schulte, "Influence of Nano-Modification on the Mechanical and Electrical Properties of Conventional Fibre-Reinforced Composites," *Composites. Part A, Applied Science and Manufacturing* 36, no. 11 (2005): 1525–1535, https://doi.org/10.1016/j.compositesa.2005.02.007.

205. N. H. Ismail, J. O. Akindoyo, and M. Mariatti, "Solvent Mediated Dispersion of Carbon Nanotubes for Glass Fibre Surface Modification—Suspensions Stability and Its Effects on Mechanical, Interlaminar and Dynamic Mechanical Properties of Modified Glass Fibre Reinforced Epoxy Laminates," *Composites Part A, Applied Science and Manufacturing* 139 (2020): 106091, https://doi.org/10.1016/j.compositesa.2020.106091.

206. L. Wang, L. Tong, S. Zhu, J. Liang, and H. Zhang, "Enhancing the Mechanical Performance of Glass Fiber-Reinforced Polymer Composites Using Multi-Walled Carbon Nanotubes," *Advanced Engineering Materials* 22, no. 8 (2020): 2000318, https://doi.org/10.1002/adem.202000318.

207. A. Haghbin, G. Liaghat, H. Hadavinia, A. M. Arabi, and M. H. Pol, "Enhancement of the Electrical Conductivity and Interlaminar Shear Strength of CNT/GFRP Hierarchical Composite Using an Electrophoretic Deposition Technique," *Materials* 10, no. 10 (2017): 1120, https://doi.org/10.3390/ma10101120.

208. F. Jamshaid, R. U. Khan, A. Islam, A. Ahmad, M. Adrees, and R. Dilshad, "Tactical Tuning of Mechanical and Thermo-Mechanical Properties of Glass Fiber/Epoxy Multi-Scale Composites by Incorporating N-(2-Aminoethyl)-3-Aminopropyl Trimethoxysilane Functionalized Carbon Nanotubes," *Iranian Polymer Journal* 29, no. 10 (2020): 875–889, https://doi.org/10.1007/s13726-020-00848-y.

209. Y. Wang, T. Chen, W. Han, et al., "Enhanced Interfacial and Mechanical Properties of Glass Fabric/Epoxy Composites via Grafting Silanized Carbon Nanotubes Onto the Fibers," *Polymer Composites* 44, no. 9 (2023): 6027–6038, https://doi.org/10.1002/pc.27544.

210. X. J. Shen, L. X. Meng, Z. Y. Yan, et al., "Improved Cryogenic Interlaminar Shear Strength of Glass Fabric/Epoxy Composites by Graphene Oxide," *Composites Part B: Engineering* 73 (2015): 126–131, https://doi.org/10.1016/j.compositesb.2014.12.023.

211. K. Schulte and C. Baron, "Load and Failure Analyses of CFRP Laminates by Means of Electrical Resistivity Measurements," *Composites Science and Technology* 36, no. 1 (1989): 63–76, https://doi.org/10.1016/0266-3538(89)90016-X.

212. A. Todoroki and Y. Tanaka, "Delamination Identification of Cross-Ply Graphite/Epoxy Composite Beams Using Electric Resistance

15480569, 0, Downloaded from https://4spepublications.onlinelibrary.wiley.com/doi/10.1002/pc.70332, Wiley Online Library on [26/08/2025]. See the Terms and Conditions (https://onlinelibrary.wiley.com/terms-and-conditions) on Wiley Online Library for rules of use; OA articles are governed by the applicable Creative Commons License

Change Method," *Composites Science and Technology* 62 (2002): 629–639, https://doi.org/10.1016/S0266-3538(02)00013-1.

213. A. Todoroki, H. Kobayashi, and K. Matuura, "Application of Electric Potential Method to Smart Composite Structures for Detecting Delamination," *JSME International Journal Series A: Mechanics and Material Engineering* 38, no. 4 (1995): 524–530, https://doi.org/10.1299/jsmea1993.38.4_524.

214. J. C. Abry, Y. K. Choi, A. Chateauminois, B. Dalloz-Dubrujeaud, G. Giraud, and M. Salvia, "In Situ Monitoring of Damage in CFRP Laminates by Means of AC and DC Measurements," *Composites Science and Technology* 61 (2001): 855–864, https://doi.org/10.1016/S0266-3538(00)00181-0.

215. D. J. Kwon, Z. J. Wang, J. Y. Choi, P. S. Shin, K. L. Devries, and J. M. Park, "Interfacial Evaluation of Carbon Fiber/Epoxy Composites Using Electrical Resistance Measurements at Room and a Cryogenic Temperature," *Composites Part A, Applied Science and Manufacturing* 72 (2015): 160–166, https://doi.org/10.1016/j.compositesa.2015.02.007.

216. A. Todoroki, K. Omagari, Y. Shimamura, and H. Kobayashi, "Matrix Crack Detection of CFRP Using Electrical Resistance Change With Integrated Surface Probes," *Composites Science and Technology* 66 (2006): 1539–1545, https://doi.org/10.1016/j.compscitech.2005.11.029.

217. D. Y. Song, N. Takeda, and A. Kitano, "Correlation Between Mechanical Damage Behavior and Electrical Resistance Change in CFRP Composites as a Health Monitoring Sensor," *Materials Science and Engineering A* 456, no. 1 (2007): 286–291, https://doi.org/10.1016/j.msea.2006.11.130.

218. A. Todoroki, T. Miho, S. Yoshinobu, and H. Kobayashi, "Effects With a Matrix Crack on Monitoring by Electrical Resistance Method," *Advanced Composite Materials* 13, no. 2 (2004): 107–120, https://doi.org/10.1163/1568551041718071.

219. T. J. Swait, F. R. Jones, and S. A. Hayes, "A Practical Structural Health Monitoring System for Carbon Fibre Reinforced Composite Based on Electrical Resistance," *Composites Science and Technology* 72, no. 13 (2012): 1515–1523, https://doi.org/10.1016/j.compscitech.2012.05.022.

220. D. D. L. Chung, "A Critical Review of Piezoresistivity and Its Application in Electrical-Resistance-Based Strain Sensing," *Journal of Materials Science* 55, no. 32 (2020): 15367–15396, https://doi.org/10.1007/s10853-020-05099-z.

221. M. Kupke, K. Schulte, and R. Schüler, "Non-Destructive Testing of FRP by d.c. and a.c. Electrical Methods," *Composites Science and Technology* 61, no. 6 (2001): 837–847, https://doi.org/10.1016/S0266-3538(00)00180-9.

222. J. Wen, Z. Xia, and F. Choy, "Damage Detection of Carbon Fiber Reinforced Polymer Composites via Electrical Resistance Measurement," *Composites, Part B: Engineering* 42, no. 1 (2011): 77–86, https://doi.org/10.1016/j.compositesb.2010.08.005.

223. K. Schulte, S. Chandrasekaran, C. Viets, and B. Fiedler, "New Functions in Polymer Composites Using a Nanoparticle-Modified Matrix," in *Multifunctionality of Polymer Composites: Challenges and New Solutions* (William Andrew Publishing, 2015), 875–902, https://doi.org/10.1016/B978-0-323-26,434-1.00030-1.

224. M. Zappalorto, F. Panozzo, P. A. Carraro, and M. Quaresimin, "Electrical Response of a Laminate With a Delamination: Modelling and Experiments," *Composites Science and Technology* 143 (2017): 31–45, https://doi.org/10.1016/j.compscitech.2017.02.023.

225. V. Kostopoulos, A. Vavouliotis, P. Karapappas, P. Tsotra, and A. Paipetis, "Damage Monitoring of Carbon Fiber Reinforced Laminates Using Resistance Measurements. Improving Sensitivity Using Carbon Nanotube Doped Epoxy Matrix System," *Journal of Intelligent Material Systems and Structures* 20, no. 9 (2009): 1025–1034, https://doi.org/10.1177/1045389X08099993.

226. M. H. G. Wichmann, J. Sumfleth, F. H. Gojny, M. Quaresimin, B. Fiedler, and K. Schulte, "Glass-Fibre-Reinforced Composites With Enhanced Mechanical and Electrical Properties—Benefits and Limitations of a Nanoparticle Modified Matrix," *Engineering Fracture Mechanics* 73, no. 16 (2006): 2346–2359, https://doi.org/10.1016/j.engfracmech.2006.05.015.

227. E. T. Thostenson and T. W. Chou, "Carbon Nanotube Networks: Sensing of Distributed Strain and Damage for Life Prediction and Self Healing," *Advanced Materials* 18, no. 21 (2006): 2837–2841, https://doi.org/10.1002/adma.200600977.

228. N. D. Alexopoulos, C. Bartholome, P. Poulin, and Z. Marioli-Riga, "Structural Health Monitoring of Glass Fiber Reinforced Composites Using Embedded Carbon Nanotube (CNT) Fibers," *Composites Science and Technology* 70, no. 2 (2010): 260–271, https://doi.org/10.1016/j.compscitech.2009.10.017.

229. N. Yamamoto, R. Guzman de Villoria, and B. L. Wardle, "Electrical and Thermal Property Enhancement of Fiber-Reinforced Polymer Laminate Composites Through Controlled Implementation of Multi-Walled Carbon Nanotubes," *Composites Science and Technology* 72, no. 16 (2012): 2009–2015, https://doi.org/10.1016/j.compscitech.2012.09.006.

230. D. Zhang, L. Ye, D. Wang, Y. Tang, S. Mustapha, and Y. Chen, "Assessment of Transverse Impact Damage in GF/EP Laminates of Conductive Nanoparticles Using Electrical Resistivity Tomography," *Composites. Part A, Applied Science and Manufacturing* 43, no. 9 (2012): 1587–1598, https://doi.org/10.1016/j.compositesa.2012.04.012.

231. J. Rausch and E. Mäder, "Health Monitoring in Continuous Glass Fibre Reinforced Thermoplastics: Tailored Sensitivity and Cyclic Loading of CNT-Based Interphase Sensors," *Composites Science and Technology* 70, no. 13 (2010): 2023–2030, https://doi.org/10.1016/j.compscitech.2010.08.003.

232. L. Vertuccio, V. Vittoria, L. Guadagno, and F. De Santis, "Strain and Damage Monitoring in Carbon-Nanotube-Based Composite Under Cyclic Strain," *Composites. Part A, Applied Science and Manufacturing* 71 (2015): 9–16, https://doi.org/10.1016/j.compositesa.2015.01.001.

233. X. Zeng, S. Yu, R. Sun, and J. b. Xu, "Mechanical Reinforcement While Remaining Electrical Insulation of Glass Fibre/Polymer Composites Using Core–Shell CNT@SiO2 Hybrids as Fillers," *Composites Part A, Applied Science and Manufacturing* 73 (2015): 260–268, https://doi.org/10.1016/j.compositesa.2015.03.015.

234. L. Böger, M. H. G. Wichmann, L. O. Meyer, and K. Schulte, "Load and Health Monitoring in Glass Fibre Reinforced Composites With an Electrically Conductive Nanocomposite Epoxy Matrix," *Composites Science and Technology* 68, no. 7 (2008): 1886–1894, https://doi.org/10.1016/j.compscitech.2008.01.001.

235. L. Gao, E. T. Thostenson, Z. Zhang, and T. W. Chou, "Sensing of Damage Mechanisms in Fiber-Reinforced Composites Under Cyclic Loading Using Carbon Nanotubes," *Advanced Functional Materials* 19, no. 1 (2009): 123–130, https://doi.org/10.1002/adfm.200800865.

236. L. Gao, E. T. Thostenson, Z. Zhang, and T. W. Chou, "Coupled Carbon Nanotube Network and Acoustic Emission Monitoring for Sensing of Damage Development in Composites," *Carbon* 47, no. 5 (2009): 1381–1388, https://doi.org/10.1016/j.carbon.2009.01.030.

237. P. C. Ma, N. A. Siddiqui, G. Marom, and J. K. Kim, "Dispersion and Functionalization of Carbon Nanotubes for Polymer-Based Nanocomposites: A Review," *Composites. Part A, Applied Science and Manufacturing* 41, no. 10 (2010): 1345–1367, https://doi.org/10.1016/j.compositesa.2010.07.003.

238. C. Viets, S. Kaysser, and K. Schulte, "Damage Mapping of GFRP via Electrical Resistance Measurements Using Nanocomposite Epoxy Matrix Systems," *Composites, Part B: Engineering* 65 (2014): 80–88, https://doi.org/10.1016/j.compositesb.2013.09.049.

15480569, 0, Downloaded from https://4spepublications.onlinelibrary.wiley.com/doi/10.1002/pc.70332, Wiley Online Library on [26/08/2025]. See the Terms and Conditions (https://onlinelibrary.wiley.com/terms-and-conditions) on Wiley Online Library for rules of use; OA articles are governed by the applicable Creative Commons License

239. M. Felisberto, L. Tzounis, L. Sacco, et al., "Carbon Nanotubes Grown on Carbon Fiber Yarns by a Low Temperature CVD Method: A Significant Enhancement of the Interfacial Adhesion Between Carbon Fiber/Epoxy Matrix Hierarchical Composites," *Composites Communications* 3 (2017): 33–37, https://doi.org/10.1016/j.coco.2017.01.003.

240. N. Wiegand, M. Haupt, E. Mäder, and C. Cherif, "A Comparative Study on the Textile Processing of Carbon and Multifunctional Glass Fiber Sensor Yarns for Structural Health Monitoring," *Advanced Engineering Materials* 18, no. 3 (2016): 385–390, https://doi.org/10.1002/adem.201500449.

241. K. Tsirka, G. Foteinidis, K. Dimos, L. Tzounis, D. Gournis, and A. S. Paipetis, "Production of Hierarchical All Graphitic Structures: A Systematic Study," *Journal of Colloid and Interface Science* 487 (2017): 444–457, https://doi.org/10.1016/j.jcis.2016.10.075.

242. L. Gao, T. W. Chou, E. T. Thostenson, A. Godara, Z. Zhang, and L. Mezzo, "Highly Conductive Polymer Composites Based on Controlled Agglomeration of Carbon Nanotubes," *Carbon* 48, no. 9 (2010): 2649–2651, https://doi.org/10.1016/j.carbon.2010.03.027.

243. B. Hao and P. C. Ma, "Chapter 3—Carbon Nanotubes for Defect Monitoring in Fiber-Reinforced Polymer Composites," in *Industrial Applications of Carbon Nanotubes*, ed. H. Peng, Q. Li, and T. Chen (Elsevier, 2017), 71–99, https://doi.org/10.1016/B978-0-323-41481-4.00003-4.

244. L. Tzounis, M. Zappalorto, F. Panozzo, et al., "Highly Conductive Ultra-Sensitive SWCNT-Coated Glass Fiber Reinforcements for Laminate Composites Structural Health Monitoring," *Composites Part B: Engineering* 169 (2019): 37–44, https://doi.org/10.1016/j.compositesb.2019.03.070.

245. T. Yamane, T. Akira, F. Hiroyasu, K. Ai, and N. Sekine, "Electric Current Distribution of Carbon Fiber Reinforced Polymer Beam: Analysis and Experimental Measurements," *Advanced Composite Materials* 25, no. 6 (2016): 497–513, https://doi.org/10.1080/09243046.2015.1126665.

246. X. Wang and D. D. L. Chung, "Continuous Carbon Fibre Epoxy-Matrix Composite as a Sensor of Its Own Strain," *Smart Materials and Structures* 5, no. 6 (1996): 796–800, https://doi.org/10.1088/0964-1726/5/6/009.

247. J. C. Abry, S. Bochard, A. Chateauminois, M. Salvia, and G. Giraud, "In Situ Detection of Damage in CFRP Laminates by Electrical Resistance Measurements," *Composites Science and Technology* 59, no. 6 (1999): 925–935, https://doi.org/10.1016/S0266-3538(98)00132-8.

248. A. Todoroki and J. Yoshida, "Electrical Resistance Change of Unidirectional CFRP due to Applied Load," *JSME International Journal Series A Solid Mechanics and Material Engineering* 47, no. 3 (2004): 357–364, https://doi.org/10.1299/jsmea.47.357.

249. S. Wang and D. D. L. Chung, "Negative Piezoresistivity in Continuous Carbon Fiber Epoxy-Matrix Composite," *Journal of Materials Science* 42, no. 13 (2007): 4987–4995, https://doi.org/10.1007/s10853-006-0580-z.

250. A. Todoroki and J. Yoshida, "Apparent Negative Piezoresistivity of Single-Ply CFRP due to Poor Electrical Contact of Four-Probe Method," *Key Engineering Materials* 297 (2005): 610–615, https://doi.org/10.4028/www.scientific.net/KEM.297-300.610.

251. N. Angelidis, C. Y. Wei, and P. E. Irving, "The Electrical Resistance Response of Continuous Carbon Fibre Composite Laminates to Mechanical Strain," *Composites. Part A, Applied Science and Manufacturing* 35, no. 10 (2004): 1135–1147, https://doi.org/10.1016/j.compositesa.2004.03.020.

252. K. Almuhammadi, L. Selvakumaran, M. Alfano, Y. Yang, T. K. Bera, and G. Lubineau, "Laser-Based Surface Preparation of Composite Laminates Leads to Improved Electrodes for Electrical Measurements," *Applied Surface Science* 359 (2015): 388–397, https://doi.org/10.1016/j.apsusc.2015.10.086.

253. A. Todoroki, K. Suzuki, Y. Mizutani, and R. Matsuzaki, "Durability Estimates of Copper Plated Electrodes for Self-Sensing CFRP Composites," *Journal of Solid Mechanics and Materials Engineering* 4, no. 6 (2010): 610–620, https://doi.org/10.1299/jmmp.4.610.

254. E. B. Jeon, T. Fujimura, K. Takahashi, and H. S. Kim, "An Investigation of Contact Resistance Between Carbon Fiber/Epoxy Composite Laminate and Printed Silver Electrode for Damage Monitoring," *Composites. Part A, Applied Science and Manufacturing* 66 (2014): 193–200, https://doi.org/10.1016/j.compositesa.2014.08.002.

255. Y. Nishio, A. Todoroki, Y. Mizutani, Y. Suzuki, M. Mitsue, and T. Nakaoka, "J0440402 Laser Treatment of Surface Resin in the Manufacturing Process of Electrodes for Self-Sensing CFRP," *Proceedings of Mechanical Engineering Congress, Japan* 2015 (2015): J0440402, https://doi.org/10.1299/jsmemecj.2015._J0440402.

256. P. E. Irving and C. Thiagarajan, "Fatigue Damage Characterization in Carbon Fibre Composite Materials Using an Electrical Potential Technique," *Smart Materials and Structures* 7, no. 4 (1998): 456–466, https://doi.org/10.1088/0964-1726/7/4/004.

257. X. Wang and D. D. L. Chung, "Sensing Delamination in a Carbon Fiber Polymer-Matrix Composite During Fatigue by Electrical Resistance Measurement," *Polymer Composites* 18, no. 6 (1997): 692–700, https://doi.org/10.1002/pc.10322.

258. T. Prasse, F. Michel, G. Mook, K. Schulte, and W. Bauhofer, "A Comparative Investigation of Electrical Resistance and Acoustic Emission During Cyclic Loading of CFRP Laminates," *Composites Science and Technology* 61, no. 6 (2001): 831–835, https://doi.org/10.1016/S0266-3538(00)00179-2.

259. A. Todoroki, K. Omagari, and M. Ueda, "Matrix Crack Detection of CFRP Laminates in Cryogenic Temperature Using Electrical Resistance Change Method," *Key Engineering Materials* 321 (2006): 873–876, https://doi.org/10.4028/www.scientific.net/KEM.321-323.873.

260. A. Todoroki and K. Omagari, "Detection of Matrix Crack Density of CFRP Using an Electrical Potential Change Method With Multiple Probes," *Journal of Solid Mechanics and Materials Engineering* 2, no. 6 (2008): 718–729, https://doi.org/10.1299/jmmp.2.718.

261. T. Augustin, G. Danny, H. L. Hauke, H. Vico, and B. Fiedler, "Online Monitoring of Surface Cracks and Delaminations in Carbon Fiber/Epoxy Composites Using Silver Nanoparticle Based Ink," *Advanced Manufacturing: Polymer & Composites Science* 3, no. 3 (2017): 110–119, https://doi.org/10.1080/20550340.2017.1362508.

262. F. Panozzo, M. Zappalorto, L. Maragoni, S. K. Nothdurfter, A. Rullo, and M. Quaresimin, "Modelling the Electrical Resistance Change in a Multidirectional Laminate With a Delamination," *Composites Science and Technology* 162 (2018): 225–234, https://doi.org/10.1016/j.compscitech.2018.04.031.

263. C. Fischer and F. J. Arendts, "Electrical Crack Length Measurement and the Temperature Dependence of the Mode I Fracture Toughness of Carbon Fibre Reinforced Plastics," *Composites Science and Technology* 46, no. 4 (1993): 319–323, https://doi.org/10.1016/0266-3538(93)90177-I.

264. Y. Ngabonziza, H. Ergun, R. Kuznetsova, et al., "An Experimental Study of Self-Diagnosis of Interlaminar Damage in Carbon-Fiber Composites," *Journal of Intelligent Material Systems and Structures* 21, no. 3 (2009): 233–242, https://doi.org/10.1177/1045389X09347019.

265. H. D. Roh, S. Y. Lee, E. Jo, H. Kim, W. Ji, and Y. B. Park, "Deformation and Interlaminar Crack Propagation Sensing in Carbon Fiber Composites Using Electrical Resistance Measurement," *Composite Structures* 216 (2019): 142–150, https://doi.org/10.1016/j.compstruct.2019.02.100.

266. A. Todoroki, M. Tanaka, and Y. Shimamura, "Measurement of Orthotropic Electric Conductance of CFRP Laminates and Analysis of the Effect on Delamination Monitoring With an Electric Resistance

15480569, 0, Downloaded from https://4spepublications.onlinelibrary.wiley.com/doi/10.1002/pc.70332, Wiley Online Library on [26/08/2025]. See the Terms and Conditions (https://onlinelibrary.wiley.com/terms-and-conditions) on Wiley Online Library for rules of use; OA articles are governed by the applicable Creative Commons License

Change Method," *Composites Science and Technology* 62, no. 5 (2002): 619–628, https://doi.org/10.1016/S0266-3538(02)00019-2.

267. A. Todoroki, "The Effect of Number of Electrodes and Diagnostic Tool for Monitoring the Delamination of CFRP Laminates by Changes in Electrical Resistance," *Composites Science and Technology* 61, no. 13 (2001): 1871–1880, https://doi.org/10.1016/S0266-3538(01)00088-4.

268. A. Todoroki, "Electric Current Analysis of CFRP Using Perfect Fluid Potential Flow," *Transactions of the Japan Society for Aeronautical and Space Sciences* 55, no. 3 (2012): 183–190, https://doi.org/10.2322/tjsass.55.183.

269. A. Todoroki and M. Arai, "Simple Electric-Voltage-Change-Analysis Method for Delamination of Thin CFRP Laminates Using Anisotropic Electric Potential Function," *Advanced Composite Materials* 23, no. 3 (2014): 261–273, https://doi.org/10.1080/09243046.2013.851357.

270. A. Todoroki, "New Analytical Method for Electric Current and Multiple Delamination Cracks for Thin CFRP Cross-Ply Laminates Using Equivalent Electric Conductance," *Advanced Composite Materials* 25, no. 1 (2016): 87–101, https://doi.org/10.1080/09243046.2014.985420.

271. T. Yamane and A. Todoroki, "Doublet Analysis of Changes in Electric Potential Induced by Delamination Cracks in Carbon-Fiber-Reinforced Polymer Laminates," *Composite Structures* 176 (2017): 217–224, https://doi.org/10.1016/j.compstruct.2017.05.019.

272. P. A. Carraro, A. Pontefisso, F. Panozzo, M. Quaresimin, and M. Zappalorto, "Health Monitoring of Bonded Joints Through Electrical Measurements," *Structural Health Monitoring* (2024): 14759217241264928, https://doi.org/10.1177/14759217241264928.

15480569, 0, Downloaded from https://4spepublications.onlinelibrary.wiley.com/doi/10.1002/pc.70332, Wiley Online Library on [26/08/2025]. See the Terms and Conditions (https://onlinelibrary.wiley.com/terms-and-conditions) on Wiley Online Library for rules of use; OA articles are governed by the applicable Creative Commons License